FAST/Polar Conjunction Study of Field-Aligned Auroral Acceleration and Corresponding Magnetotail Drivers

D. Schriver[1], M. Ashour-Abdalla[1,2], R.J. Strangeway[1], R.L. Richard[1], C. Klezting[3], Y. Dotan[4], and J. Wygant[5]

[1]Institute of Geophysics and Planetary Physics, University of California at Los Angeles, Los Angeles, California

[2]Department of Physics and Astronomy, University of California at Los Angeles, Los Angeles, California

[3]Department of Physics, University of Iowa, Iowa City, Iowa

[4]Aerospace Corporation, Los Angeles, California

[5]University of Minnesota, Minneapolis, Minnesota

Abstract

The discrete aurora results when energized electrons bombard the Earth's atmosphere at high latitudes. This paper examines the physical processes that can cause field-aligned acceleration of plasma particles in the auroral region. A data and theoretical study has been carried out to examine the acceleration mechanisms that operate in the auroral zone and to identity the magnetospheric drivers of these acceleration mechanisms. The observations used in the study were collected by the Fast Auroral SnapshoT (FAST) and Polar satellites when the two satellites were in approximate magnetic conjunction in the auroral region. During these events FAST was in the middle of the auroral zone and Polar was above the auroral zone in the near-Earth plasma sheet. Polar data was used to determine the conditions in the magnetotail at the time field-aligned acceleration was measured by FAST in the auroral zone. For each of the magnetotail drivers identified in the data study, the physics of field-aligned acceleration in the auroral region was examined using existing theoretical efforts and a long-system particle-in-cell simulation to model the magnetically connected region between the two satellites. Results from the study indicate that there are three main acceleration mechanisms operating in the auroral zone: (1) quasi-static potential drops (parallel electric fields) that form in regions of field-aligned

current, (2) relatively strong quasi-static parallel potential drops formed by the inflow of high energy plasma from the magnetotail, and (3) kinetic Alfvén waves with a parallel electric field component that propagates into the auroral region from the magnetotail. The occurrence of the drivers and particular acceleration characteristics depends mainly on magnetic activity. During quiet times, field-aligned currents are the only driver present and earthward electron acceleration is relatively weak with no upwelling ions observed. During more active times, earthward propagating magnetotail particle beams and Alfvén waves appear along with field-aligned currents, and in addition to more intense bursty earthward electron acceleration, upwelling ion beams flowing tailward are observed. The results presented here give support to the overall contention that while processes in the magnetotail lead to the discrete aurora, it is not a single process, but several processes acting at different locations and different times.

1. Introduction

The visual light display at high latitudes referred to as the aurora fascinates casual observers and researchers alike. The natural question is what causes the aurora? We know that energized electrons streaming along the Earth's ambient magnetic field and colliding with atmospheric particles produce aurora. We do not know for certain, however, how these electrons are accelerated to high energies primarily in the field-aligned direction toward the Earth, or what the drivers of this acceleration are.

It has been known for some time that field-aligned accelerated precipitating electrons can cause discrete aurora. Key evidence from rocket and satellite observations made above the aurora show the presence of energetic, field-aligned electron distributions streaming earthward as well as back-scattered secondary electrons. [*McIlwain*, 1960; *Hoffman and Evans*, 1968; *Hultqvist et al.*, 1971; *Frank and Ackerson*, 1971; *Rees and Luckey*, 1974; *Evans*, 1974; *Christensen et al.*, 1987]. It should be noted that discrete aurora and diffuse aurora are two different phenomena. Diffuse aurora is also caused by electron precipitation, but it results from the emptying of the loss cone of mirror bouncing plasma sheet electron distributions, which give rise to a broader, less intense aurora. The refilling of the loss cone is believed to be caused by wave-particle pitch angle diffusion at the magnetotail equator [*Kennel and Petschek*, 1966; *Kennel*, 1969]. This paper only addresses the causes of the discrete aurora.

Although it is well established that energized, precipitating electrons create the discrete aurora, no general consensus exists regarding how these electrons achieve such energies and become focused mainly in the field-aligned direction. There are two main acceleration processes that are considered likely to occur in the auroral zone:

(1) Quasi-static parallel potential drops (parallel electric fields) that can occur in regions of field-aligned current near the Earth above the ionosphere where densities are relatively low and the magnetic mirror force is relatively strong [e.g., *Knight*, 1973]. Quasi-static parallel potential drops can also form when pitch angle anisotropies (a beam and/or temperature anisotropy) in magnetotail plasma sheet distribution functions lead to differing mirror points of ions and electrons and a resulting charge separation [*Alfvén and Fälthammer*, 1963; *Persson*, 1963]. Many models of a steady-state auroral electrostatic potential drop have been developed based on one or the other of these basic premises [e.g., *Lemaire and Scherer,* 1974; *Swift,* 1975; *Kan,* 1975; *Whipple,* 1977, *Chiu and Cornwall,* 1980].

(2) A parallel electric field component of a kinetic Alfvén wave can develop near the Earth because of finite electron inertia [e.g., *Hasegawa*, 1976; *Mallinckrodt and Carlson*, 1978; *Goertz and Boswell*, 1979; *Lysak,* 1985]. On electron time scales this parallel field can appear quasi-static and due to resonance and other effects can cause field-aligned electron acceleration [*Temerin et al.*, 1986; *Kletzing*, 1994; *Thompson and Lysak*, 1996].

Although the two auroral acceleration mechanisms, parallel potential drops and kinetic Alfvén waves, each involve a parallel electric field, they are fundamentally different in that the former is primarily electrostatic and the latter is an electromagnetic wave. It has been suggested that for small spatial scales electrostatic shocks might be a manifestation of an inertial Alfvén wave, however, on larger scales the two mechanisms appear to be unrelated [*Lysak*, 1998].

It is likely that auroral acceleration is ultimately due to processes occurring in the magnetotail [e.g., *Frank*, 1985; *Lyons et al.*, 1999]. The basic idea is that there is a transfer of energy from earthward propagating currents, particles and waves that originate in the magnetotail into field-aligned plasma particles in the auroral zone via a parallel potential drop

and/or kinetic Alfvén waves. It is well established that quasi-static (dc) parallel electric fields (inverted V structures and parallel potential drops) occur in regions of field-aligned current [*Mozer et al.*, 1977; *Elphic et al.*, 1998], which map into the magnetotail where they presumably originate as part of the global magnetospheric current system [e.g., *Haerendel*, 1990]. In addition to the field-aligned currents, temperature anisotropies and beams have been observed at high altitudes above the auroral region [*Chiu et al.*, 1981; *Frank et al.*, 1981] that could also serve as drivers of quasi-static parallel electric fields in the aurora zone. The existence of a magnetotail driver for kinetic Alfvén wave auroral acceleration is supported by the recent observations of intense Poynting flux detected in a region above, but magnetically connected to the discrete auroral precipitation region. These observations clearly showed a field-aligned earthward propagating Poynting flux in association with Alfvén waves that had oscillating magnetic and electric field components directed primarily perpendicular to the ambient magnetic field [*Wygant et al.*, 2000; *Keiling et al.*, 2001].

In this paper, cause (magnetospheric driver) and effect (field-aligned auroral acceleration) are examined using data collected by the Fast Auroral SnapshoT (FAST) and Polar satellites when the two satellites were in approximate magnetic conjunction. In general, FAST moved through the (northern) auroral zone between about 2000 to 4000 km altitude, while Polar passed through the (northern) auroral region at much higher altitudes, between about 4 and 8 R_E. Thus when the two satellites were on approximately conjugate magnetic field lines in the northern auroral zone, Polar could determine the conditions in the magnetotail near-Earth plasma sheet at the same time that FAST was collecting data in the middle of the auroral acceleration region. There were 28 such auroral conjugate passes in 1997 between May and September. Thus far 7 events have been examined in detail. The results from examining these conjugate events are

presented here, along with a discussion of the physical processes that lead to field-aligned auroral acceleration. This includes results from a simulation model of the region between the two satellites carried out with a long-system PIC code [*Schriver*, 1999; 2002]. Simulation boundary conditions at the high altitude end of the system were set (qualitatively) for one of the events using measurements from the Polar satellite, and the simulation results were compared with observational data.

The fortunate alignment and relative locations (in altitude) of the FAST and Polar satellites allow a thorough analysis of magnetotail-aurora cause and effect. A similar type of study was previously carried out for the auroral zone using the DE-1 and DE-2 satellites. In that case the measurement of precipitating auroral electrons at low altitudes (with DE-2), along with simultaneously observed upwelling ion beams at higher altitudes (with DE-1), indicated that a quasi-static (at least on ion time scales) parallel potential drop existed between the two satellites [*Reiff et al.*, 1986; 1988]. No attempt was made in those studies to determine a magnetotail driver of the parallel potential drop. In this study, in addition to the improved instrumentation, Polar and FAST were at near-optimum locations to determine cause and effect since FAST observed the middle of the auroral acceleration region at a few thousand kilometers altitude, whereas Polar was well above the acceleration region in the near-Earth plasma sheet ($> 4\ R_E$). By comparison DE-2 and DE-1 were at altitudes of 400 to 800 km and 9000 to 13000 km, respectively.

Seven FAST/Polar conjugate events have been examined in detail thus far. All seven events showed field-aligned electron precipitation in regions of field-aligned currents. Three of the events that occurred during moderate magnetically active intervals indicated that, in addition to a field-aligned current, a magnetotail Poynting flux driver (Alfvén wave) was present. During

two events with the highest magnetic activity level a magnetotail particle flux driver (quasi-static potential drop accelerator) was also present. Four events during quiet times showed only the field-aligned current driver (quasi-static potential drop accelerator) at Polar. Not only could each driver accelerate electrons earthward, some were correlated with tailward plasma acceleration. For example, tailward streaming electrons were found in some cases in which Alfvén waves were present or in the return (earthward directed) field-aligned current region. Tailward streaming ions, however, were found only when the magnetotail particle flux driver was present or at certain times in regions of a strong primary (tailward directed) field-aligned current region. During events in which a field-aligned current was the only identifiable driver, only earthward accelerated electrons were detected (with relatively low energies) and there were no tailward streaming ions. Most of these results are consistent with the physics of the driver involved. For example, if low frequency (~ 1 Hz) kinetic Alfvén waves are present in the auroral region, electrons would see a quasi-static parallel electric field and could be accelerated, whereas ions would see a fluctuating field and would not be accelerated in the field-aligned direction. A particle flux driver or strong field-aligned current, on the other hand, can lead to a quasi-static parallel potential drop in the auroral zone that can accelerate electrons earthward and ions tailward. Field-aligned currents can lead to the formation of a quasi-static potential drop that accelerates electrons earthward and although ions would be expected to be accelerated tailward, observations did not show this to be the case for the four quiet events. In those events the field-aligned current was relatively weak and it is possible that if the potential drop is in the form of a weak double layer, the upwelling ion beams were not created.

The results of this study are presented in the following structure. In section 2, FAST/Polar satellite data conjunction criteria and event selection are presented, and section 3 discusses a

single event in detail. Section 4 analyzes the physics of auroral acceleration discussing cause and effect relationships and simulation modeling. Section 5 summarizes all of the events examined so far, and the paper concludes in section 6.

2. Polar/FAST Conjugate Events

This study examined data from measurements taken when the FAST and Polar satellites were in approximate magnetic conjunction. A list of magnetic conjunctions between FAST and Polar can be found at ftp://sierra.spasci.com/DATA/fast/prior_conjunctions_1.html, which has been compiled by William Peterson. In that list, a magnetic conjunction was defined to occur when the satellites were within 3 degrees in invariant latitude (ILT) and within 10 degrees in longitude. Magnetic field mapping between the two satellites was carried out using the Tsyganenko field model [*Tsyganenko*, 1989], which near the earth uses an IGRF internal magnetic field. Figure 1 shows an example of an auroral conjugate event that occurred on June 9, 1997. The figure presents the track of the FAST satellite in red, the Polar satellite in blue-white, and the nominal auroral oval as green circles. These lines are projected onto the Earth looking down on the North Pole, and conjunction occurred where the red and white lines cross at about 04:32 UT. A two-dimensional schematic with the relative locations of the FAST and Polar flight paths near conjunction along with auroral latitude field lines is shown in figure 2. Note that this event (June 9, 1997) is discussed in detail in section 3. For all of the conjunction events examined here, the FAST satellite was located between about 2000 and 4000 kilometers altitude, while Polar was at relatively higher latitudes between about 4 and 8 R_E (1 $R_E \approx 6371$ km) in the northern hemisphere. During the single southern hemisphere auroral conjugate event that was found, FAST was located at about 400 km altitude and Polar at about 2.1 R_E.

In 1997, FAST and Polar satisfied the conditions for a magnetic conjugate event hundreds of times. For example, during the period between July 20, 1997 and September 8, 1997, the two satellites satisfied the conjugacy criteria almost 120 times. Only a select number of these events, however, occurred when the two satellites were in the closed-field line region of the auroral zone, and when data was available from both satellites. Events that were not of interest to the present study, and thus were not examined, included polar cap crossings, lower latitude crossings, most southern hemisphere crossings, and events for which data was not available for both satellites.

For this study, an auroral acceleration event was selected when FAST particle data showed energetic field-aligned electrons with a net earthward flow. A description of the FAST mission can be found in *Carlson et al.* [1998a]. An example of such an auroral acceleration event from July 20, 1997 is shown in figure 3. The top two panels of figure 3 show electron energy and electron pitch angle, and a somewhat sporadic group of acceleration occurrences can be seen between about 16:21 and 16:26 UT as bright red spots at 0° pitch angle (middle panel) with energies between about 100 and 1000 eV (top panel). The direction of 0° pitch angle is field-aligned toward the Earth, while 180° is field-aligned away from the Earth. The bottom panel shows the magnetic field with the field-aligned component (b) in blue, the east-west component (e) in green and the component transverse to these two components (o) in red. The overall increase in the east-west component (green line) indicates the satellite is flying through a region of field-aligned current with the initial negative depression corresponding to an upward, region 2 sense current on the dawn side followed by a region 1 current directed earthward. There are sharp changes imbedded in the overall current structure that show localized smaller scale reversals of the field-aligned current. For this event, magnetic conjugacy between FAST and

Polar occurred at about 16:24 UT. Events were used for this study for which FAST showed clear evidence of energetic electrons streaming earthward during near-conjunctions of FAST and Polar as shown in figure 3.

Once an auroral acceleration conjugate event was identified, additional data from FAST was obtained (particle, wave and field data), and similar data was obtained from Polar. The Hydra instrument on Polar [*Scudder et al.*, 1995] provided particle data with energies below 32 keV. For higher energies (> 30 keV) particle data from the CEPPAD instrument [*Blake et al.*, 1995] was used. Electric field data [*Harvey et al.*, 1995] and magnetic field data [*Russell et al.*, 1995] from Polar were also examined. Our main goal is use particle and field data from Polar to determine what causes the earthward-directed field-aligned acceleration seen at FAST altitudes.

3. Event Case Study: June 9, 1997

This section presents a single event case study to demonstrate the type of analysis carried out for the conjunction events. Data from an auroral conjunction event that occurred on June 9, 1997 at about 04:32 UT will be used for this case study. It should be noted that, while other events similar to this one have been found, this event occurred near the peak of a moderate magnetic storm event with Dst at a minimum of -84 nT (as determined by the WDC-C2 KYOTO final Dst index service at: http://swdcdb.kugi.kyoto-u.ac.jp/dstdir/dst1/final.html). At 04:32 UT, FAST (orbit 3155) was located at about 2500 km altitude, 71° ILT and 20.3 MLT. Polar (orbit 160) was located at 3.9 R_E altitude, 71° ILT, and 19.8 MLT. The relative locations of the two satellites for this event are shown in figures 1 and 2.

FAST data from this event is presented in figure 4 showing electron energy and pitch angle in the top two panels and magnetic field in the bottom panel in the same format as figure 3. Earthward directed field-aligned acceleration is indicated in the middle panel by the intermittent

red bursts centered at 0^o pitch angle from about 04:31:30 UT to just after 04:33 UT. The energies of the field-aligned electron bursts are about 1 keV (~ 1000 eV in the top panel). The energy flux of the downgoing (precipitating) accelerated electrons ranges from about 1 to 10 ergs/cm^{2}s. This measured energy flux is of the order of that previously reported to occur in auroral arcs [*Elphic et al.*, 1998; *Stenbaek-Nielsen et al.*, 1998]. In particular, close to the conjunction at about 04:32 UT, there is a field-aligned electron burst with energy of the order of 1 keV. Prior to about 04:31:30 UT, FAST is in the polar cap, which can be inferred from the lack of high-energy electrons (> 100 eV). FAST then crosses into a region of field-aligned current, as indicated by the overall increase in the east-west magnetic field component (green line, bottom panel). Since FAST is on the dusk side, the increase in east-west field component indicates a tailward-directed region 1 sense current, which is labeled as FAC- between the middle and bottom panels. The east-west magnetic field decreases after about 04:32:30 UT indicating that FAST is passing through the return field-aligned current region, which is directed earthward along the terrestrial magnetic field direction and indicated by FAC+. There are smaller scale current structures embedded onto the overall field-aligned current system (region 1 and return current) that in some cases correspond with the field-aligned electron bursts.

Comparison of the earthward streaming field-aligned bursts with the field-aligned currents as determined from the magnetic field in figure 4 shows two interesting features that will be important when looking at the magnetospheric drivers with Polar. One, as already noted, is that in the upward directed region 1 current (~ 04:31:30 UT to ~ 04:32:30 UT), the field-aligned electrons are not continuous in the larger-scale current structure, but instead are bursty. The second is that energetic field-aligned earthward streaming electrons are observed even in the return current region (after ~ 04:32:30 UT) where the field-aligned current is directed earthward.

It should be noted that the intermittent bursts of earthward accelerated electrons are a common feature in the electron data and have been seen in other auroral conjunction events (e.g., figure 3).

The electron data shown in figure 4 clearly indicate that electrons have been accelerated earthward in the field-aligned direction at some location above the satellite. An example of an electron distribution function near conjunction (~ 04:32 UT) is presented in figure 5, which shows distribution contours plotted in the perpendicular direction (vertical) and parallel direction (horizontal). Positive parallel velocities correspond to the earthward direction. The most obvious feature is the elongation of the velocity contours in the parallel earthward direction, corresponding to the peak at 0^{o} pitch angle seen in figure 4. It is interesting to note that, even though there is clearly a net electron flow in the earthward direction along the magnetic field, there is no distinct beam present in the distribution. This is probably because the electrons are preferentially accelerated in the field-aligned direction at some location above the satellite and form a beam. This beam then excites plasma waves that smear the beam distribution via wave-particle interactions. Electric field data at this time (not shown) indicates the presence of electrostatic oscillations near the upper hybrid frequency, which would be consistent with a beam driven instability. Although beam-generated waves in the auroral zone are themselves interesting, they are beyond the scope of the present paper.

The goal of this study is to determine the field-aligned electron acceleration mechanism and the corresponding magnetotail drivers associated with this acceleration. To this end we now look at Polar data for this event, which was located above FAST along approximately the same magnetic field lines at about 3.9 R_E altitude. We start by looking at magnetic and electric field data from Polar around the time of the conjunction. Figure 6 shows the magnetic field data

observed during the time interval between 04:20 and 04:40 UT on June 9, 1997. The top panel of figure 6 shows three colored lines, which are the B_x (blue), B_y (red), and B_z (green) residual magnetic field components subtracted from the 1996 Tsyganenko field model [*Tsyganenko and Stern*, 1996] in GSM coordinates. The bottom panel shows the E_z electric field component normal to the spin plane, which corresponds approximately to the direction along z in GSE coordinates. It can be seen in figure 6 that the field profiles are relatively smooth prior to about 04:23 UT. At 04:23 UT there are strong oscillations in the magnetic and electric fields followed by a sharp decrease in the B_x field component (blue trace) until about 04:28:30 UT. After this time a gradual overall increase in B_x occurs. Note that after about 04:25 UT the electric field (bottom panel) is relatively smooth just above 0 mV/m.

The magnetic and electric field data indicate that Polar is positioned in the polar cap region at higher latitudes prior to 04:23 UT and then moves to lower latitudes crossing into a region of field-aligned current after 04:23 UT. The decreasing B_x indicates that the field-aligned current is directed away from the Earth (indicated by FAC- at the top of figure 6), which is consistent with a region 1 current system. After about 04:28:30 UT, Polar crosses through the return current region where the field-aligned current is directed earthward, as seen by the gradual increase in B_x and indicated by FAC- at the top of figure 6. This field-aligned current system is consistent with the field-aligned current system observed at low altitudes by the FAST satellite (figure 4). At Polar the field aligned current density ($j_{||}$) is estimated to be about 0.8 $\mu A/m^2$ (assuming $\Delta B_x \sim 60$ nT and $\Delta y = 50$ km), while at FAST $j_{||}$ is between about 10 to 50 times greater than at Polar (depending on the cross-field distance). This is consistent with a field-aligned current sheet that increases approximately with the terrestrial magnetic field keeping $j_{||}/B$ approximately constant

when mapped from Polar to FAST. Also, qualitatively similar to the FAST observations, are the smaller scale magnetic field structures embedded in the overall field-aligned current systems.

The other outstanding feature of the magnetic and electric fields in figure 6 (in addition to the field-aligned current systems) are the strong fluctuations that occur between about 04:23 UT and 04:25 UT. The fluctuations have a period less than 1 minute and for an electric field fluctuation amplitude of $\delta E \approx 20$ mV/m, and a magnetic field fluctuation amplitude of $\delta B \approx 15$ nT, the $\delta E/\delta B$ ratio is ~ 1300 km/s. This gives a phase speed comparable to the local Alfvén speed, which is about 1000 to 2000 km/s (using measured key parameter values at 04:24 UT of 10 cm^{-3} for the density, 425 nT for the total ambient magnetic field, and assuming a mixed hydrogen-oxygen plasma). This implies that the fluctuations correspond to an Alfvén wave, and a calculation of the Poynting flux $\mathbf{S}_{\|}$ (where $\mathbf{S}_{\|}$ is proportional to $\delta\mathbf{E} \times \delta\mathbf{B}$) shows the field aligned component is propagating earthward with an energy flux value of 0.5 to 1 erg/cm^2s. Such observations are similar to Alfvén waves previously seen by the Polar satellite in regions above the auroral zone [*Wygant et al.*, 2000; *Keiling et al.*, 2001]. This earthward propagating Poynting flux is amplified as it moves towards the Earth in proportion to the increasing magnetic field [*Wygant et al.*, 2000], and if mapped to the ionosphere would have an energy flux of the order of 100 ergs/cm^2s. The energy flux of these intense waves is quite significant and clearly represents a possible driver of field-aligned auroral acceleration and resulting electron precipitation. It should be noted, however, that for the event here the earthward propagating Alfvén waves are confined to the most poleward edge of the high-altitude auroral zone, and at lower latitudes the electric field fluctuations are near zero (after about 04:25 UT).

We now look at particle data during the same time interval from the Polar satellite Hydra instrument shown in figure 7. Electron data is given in the top two panels that show the electron

energy and electron skew. The skew is the difference in count rate between the field-aligned and the anti-field-aligned particles normalized to one-sigma error. Thus the skew is a measure of the significance of the difference between the 0°-30° and 150°-180° pitch angle bins. The skew diagrams are color-coded red for field-aligned earthward directed flow and blue for field-aligned tailward directed flow. Panels three and four (from the top) in figure 7 give the ion energy and skew in the same format as the electrons. The electrons (top panel) are relatively energetic (> 1 keV), which indicates the satellite is in the near-Earth plasma sheet or plasma sheet boundary layer (PSBL). The PSBL is a transition region between the open field-line, high latitude lobe that maps to the polar cap and the plasma sheet on closed field lines that map from the magnetotail to the auroral zone [*Eastman et al.*, 1984]. Particle data prior to 04:23 UT (not shown) confirms the satellite was in the polar cap and then crossed into the PSBL after that time (this can be seen in the magnetic field data in figure 6). The electron skew (second panel) is quite variable during the interval, however there is some indication of upflowing electrons (UFE) with energy of a few hundred eV moving in the tailward direction at about 04:34 UT to 04:35 UT corresponding to the return current region. The distribution functions that correspond to this upflowing electron event (not shown) are consistent with similar types of upflowing electrons observed previously by Polar above the auroral region [*Kletzing and Scudder*, 1999].

The ions observed by Polar during this time interval (figure 7, panels three and four) show two distinct populations with different energies. One of these ion populations can be seen at about 1 keV in the ion skew plot (panel four) as dark blue patches from 04:26 UT to 04:28 UT and again from about 04:31 UT to 04:34 UT. The skew (~ 100) of this ion population is oriented tailward and indicates an upwelling ion beam (ion distribution functions are shown in the next figure) originating from below the satellite in the auroral region. Data from the Toroidal

Imaging Mass-Angle Spectrometer (TIMAS) instrument onboard Polar shows that this upwelling population consists primarily of O^+ ions, which is a clear indicator that this population is of ionospheric origin. The second ion population has relatively higher energies between ~ 3 keV and ~ 32 keV (upper energy limit of the instrument), and can be seen most clearly in panel three as greenish regions from about 04:32 UT to 04:40 UT. These ions are mainly H^+, and their energies (> 1 keV) are consistent with PSBL plasma energies [e.g., *Frank*, 1985; *Baumjohann et al.*, 1989]. The skew of the higher energy H^+ population (yellow regions in panel four) shows an earthward directed flow, indicating that it originates from the magnetotail.

The distinct nature of these two ion populations can be more clearly seen in figure 8, which shows on the left an example of the lower energy upflowing O^+ ions at 04:32 UT and on the right the higher energy earthward flowing H^+ ions at 04:35 UT. In these plots the horizontal axis is in the field-aligned direction with positive towards the Earth and negative towards the magnetotail, and the horizontal axis is transverse to the ambient magnetic field. The left panel clearly shows a tailward drifting O^+ beam with a tailward drift speed of about −100 km/s, (which corresponds to a drift energy of about 1.7 keV). Upwelling ions are a somewhat common feature of the high altitude auroral region [*Shelley et al.*, 1976; *Ghielmetti et al.*, 1978; *Gorney et al.*, 1981; *Reiff et al.*, 1988] and are an indication of a field-aligned acceleration process at a location below the Polar satellite. The right panel shows a kidney-bean shaped ion (H^+) population with a parallel earthward drift speed of about 600 km/s (about 3.7 keV). Such a distribution function seen in the right panel of figure 8 is typical of the type of earthward streaming field-aligned ion beam distributions observed in the PSBL [*DeCoster and Frank*, 1979; *Eastman et al.*, 1984; *Takahashi and Hones*, 1988]. The field-aligned, high-energy earthward streaming ion beams are accelerated

at some location down the magnetotail in a process possibly related to tail reconnection or non-adiabatic ion motion [*Lyons and Speiser*, 1982; *Ashour-Abdalla et al.*, 1991].

The earthward streaming PSBL ion beams can act as a driver for auroral acceleration and it has been shown that these beams can lead to the formation of a quasi-static parallel potential drop in the auroral zone [e.g., *Serizawa and Sato*, 1984; *Schriver*, 1999]. The PSBL ion distribution function shown in figure 8 at 04:35 UT has a streaming energy of about 3.7 keV, but some PSBL beams during this interval have much higher energies that are above the Hydra instrument cutoff of ~ 32 keV. To examine the higher energy ions we analyzed data from the CEPPAD instrument, which has ion energy channels from 15 keV up to 1500 keV. Figure 9 shows ion count rate versus pitch angle from the CEPPAD 35.4 keV energy channel at about 04:32 UT. In figure 9 the pitch angle peaks close to 0°, which corresponds to an earthward directed flow. This feature is seen in other energy channels, and an analysis of five different energy channels (15.6 keV up to 65.2 keV) indicates that there is an earthward flowing ion distribution with a peak energy between about 35 and 45 keV. As already discussed, ion beams streaming earthward are a commonly observed feature of the PSBL [*Hones et al.*, 1972; *Frank et al.*, 1976; *Lui et al.*, 1983; *Eastman et al.*, 1984; *Takahashi and Hones*, 1988], and ion beam streaming energies up to 60 keV have been detected at the most lobeward edge of the PSBL [*Möbius et al.*, 1980; *Schriver et al.*, 1990].

We now estimate the energy flux carried by the earthward directed PSBL ion beams for the two different cases shown in figures 8 and 9. For the ion beam at 04:32 UT, an energy flux of about 0.5 to 5 ergs/cm^{2}s is estimated for a beam drift energy of 40 keV with beam density between 0.04 to 0.4 cm^{-3}. For the ion beam at 04:35 UT the energy flux is about 0.01 to 0.1 ergs/cm^{2}s for a beam drift energy of 3.7 keV and density between 0.035 to 0.35 cm^{-3}. The

biggest uncertainty in these calculations is the beam density. For example, for the PSBL beam at 04:35 UT, key parameter data from Hydra shows an electron density of the order of 0.6-0.7 cm^{-3}. TIMAS key parameter data shows that the low energy O^+ density is about 0.3-0.4 cm^{-3} and the higher energy H^+ density is about 0.30-0.35 cm^{-3}. The question to consider is how much of this H^+ density goes into making up the beam. We estimate the beam density for the energy flux calculation to range from one-tenth of the H^+ density (0.035 cm^{-3}) to the entire H^+ population (0.35 cm^{-3}). Making a similar calculation for the ion beam distribution at 04:32 UT, the electron density is somewhat higher ~ 1.0 cm^{-3}, while TIMAS (with an upper energy cutoff of ~ 32 keV) gives an O^+ density of about 0.6 cm^{-3}. Thus, assuming a PSBL H^+ beam with density of one-tenth up to the total H^+ density, the beam density is somewhere between 0.04 to 0.4 cm^{-3}.

To get an indication of the auroral activity occurring at the Earth during this event, we now show data from the Ultraviolet Imager (UVI) instrument onboard Polar [*Torr et al.,* 1995]. A plot with a view looking down onto the North Pole region of the Earth is shown in figure 10 at a time near conjunction (04:32 UT). The X in figure 10 shows the approximate location on the Earth to which the FAST/Polar locations would magnetically map on the dusk side at about 71° latitude. Enhanced auroral emissions are evident around this location, indicating enhanced electron precipitation at this time. The energy flux associated with these auroral emissions can be estimated from figure 10 by dividing the scale, which shows photons/cm^2s, by 4 [*Wygant et al.,* 2000]. With this estimate we can determine that the region with enhanced auroral emissions around conjunction has an energy flux that ranges from about 5 to 15 ergs/cm^2s. It is interesting to note that there is another auroral enhancement at lower latitudes between about 60° and 65°.

We now summarize the data from both the FAST and Polar satellites for the conjunction event on June 9, 1997 around 04:32 UT:

- A series of bursty earthward streaming field-aligned directed electrons with energies ~ 1 keV were detected at about 2500 km from about 71° to 68° with an energy flux of about 1 to 10 ergs/cm^{2}s.
- A strong region-one type field-aligned current was present from the poleward edge of the auroral region extending equatorward in latitude. The field-aligned current was observed at both low (2500 km) and high (3.9 R_E) altitudes. The field-aligned current was directed away from the Earth and sharp, small-scale variations were observed embedded in the overall field-aligned current structure. At lower latitudes towards the equator a weaker return current (field-aligned pointing earthward) was observed.
- An upwelling O^+ field-aligned beam of ionospheric origin with an energy of ~ 1 keV was observed streaming away from the Earth at about 3.9 R_E altitude. Two instances of the upwelling O^+ beams were observed: one at about 71° latitude in the primary current region and another at about 70° latitude in the return current region.
- High-energy (~ 4 keV up to 40 keV) field-aligned H^+ beams of magnetotail origin were observed streaming earthward at an altitude of 3.9 R_E between about 70° and 71° latitude. The energy flux of these beams was estimated to be about 0.5 to 5 erg/cm^{2}s.
- A relatively weak (~ 400 eV) upwelling tailward directed electron beam was observed at 3.9 R_E in the return current region.
- At the poleward edge (~ 71.5° latitude) of the high altitude (3.9 R_E) auroral region a Poynting flux due to fluctuating magnetic and electric fields (Alfvén wave) was observed propagating earthward with an energy flux of about 0.5 to 1 erg/cm^{2}s.

- Strong auroral emissions were observed in the Earth's ionosphere at locations that magnetically mapped to the FAST/Polar locations of the satellites as they passed through the auroral region.

The observations for this event allow some basic conclusions to be drawn. A field-aligned acceleration mechanism was operating at altitudes between FAST (2500 km) and Polar (3.9 R_E). This mechanism accelerated electrons earthward and O^+ ions tailward with both species having about the same streaming energy (~ 1 keV) on coincident field lines. A tailward streaming electron component was also present, although this accelerated electron population occurred at somewhat lower latitudes and with lower energies than the other field-aligned populations. Three possible magnetospheric drivers have been detected at high altitudes: (1) field-aligned currents, (2) earthward streaming PSBL ion beams, and (3) earthward propagating Alfvén waves. We now consider the physics of each of these magnetotail drivers.

4. Physics of Field-Aligned Auroral Acceleration

The magnetospheric drivers of auroral acceleration discussed in the previous section can lead to field-aligned energization of electrons and ions. To show how they relate to the conjunction event discussed in the previous section and for the event survey in the next section, we now discuss the physics of each mechanism.

4.1 Field-Aligned Current/Quasi-Static Potential Drops

It is well known on a global level that field-aligned currents form between regions of the magnetotail or magnetopause and the Earth's ionosphere at high latitudes [e.g., *Iijima and Potemra*, 1976]. The field-aligned currents originate in the magnetotail convection current sheet or the magnetopause flanks, possibly as a result of flow vortices or some other mechanism [*Vasyliunas*, 1983], flow along magnetic field lines into the Earth's ionosphere, move across the

polar cap and then return to the magnetotail. Although the precise locations and pattern of this global current structure are still being examined, there is conclusive evidence that field-aligned currents flow between the magnetosphere and the ionosphere, and that these field-aligned currents are usually located at high latitudes in coincidence with the auroral region. The event study in the previous section provides an example of such field-aligned currents in the auroral zone.

Near the Earth, where the magnetic mirror force is strong and the plasma is warm and tenuous, it is expected that a quasi-static potential drop could form according a particular current-voltage relationship [*Knight*, 1973]. For typical plasma populations in the cold, dense ionosphere and the hot, less dense plasma sheet, potential drops of several kilovolts are possible. It should be noted, however, that the *Knight* [1973] current-voltage relationship does not indicate where the potential drop should form or its extent along the terrestrial magnetic field in the auroral region. Nevertheless, to maintain current flow between the plasma sheet and the ionosphere, strong localized potential drops probably form in the primary current region of the auroral zone [e.g., *Ergun et al.*, 2000] and cause field-aligned electron acceleration towards the Earth and upwelling ion beams away from the Earth.

In the event study of the previous section a field-aligned current density of the order of 8 to 40 $\mu A/m^2$ was observed at FAST, which was located at about 2500 km altitude. Since the earthward streaming field-aligned electrons were also observed at FAST, this implies that the potential drop was located above the satellite. The potential drop ($\Delta\phi$) can be estimated using the *Knight* [1973] relationship as follows:

$$\Delta\phi = -\frac{j_{\parallel}\sqrt{2\pi mkT}}{q^2 n}$$

where m is the electron mass, n is the electron density, and T is the electron temperature. At FAST the electron density is about 100 cm^{-3} and the temperature is about 500 eV. Since the potential drop forms above the satellite and the density is known to decrease with altitude [e.g., *Kletzing and Torbert,* 1994], we use $n \sim 10$ cm^{-3}, $T \sim 500$ eV, and $j_{\|} \sim 10$ $\mu A/m^2$, which give a potential drop of $\Delta\phi \sim 850$ V. This is of the order of the energy of the earthward accelerated streaming electrons observed at FAST and the tailward streaming O^+ observed at Polar.

The field-aligned potential drop that forms due to a field-aligned current is essentially a double layer, which is defined as consisting of two equal but opposite space charge layers with a potential that varies monotonically through the layer [*Block*, 1972; 1978]. Double layers can form in a current driven plasma at the site of a density depression [*Carlqvist*, 1972], and are subject to a minimum current (Bohm) condition [*Goertz and Joyce*, 1975; *Block*, 1978]. According to this criterion, for a strong, well-defined double layer to form the net electron drift speed must be of the order of the electron thermal speed. The data suggest that this is the case for the event study of June 9, 1997, although it is difficult to verify since the satellite does not pass through the region where the potential drop forms, but below this region. In events during less active times that have been examined (to be discussed in section 5), a field-aligned current is present, although it is not nearly as strong as that found in the event study of the previous section. In those cases it would be expected that a weak double layer forms [e.g., *Eriksson and Boström*, 1993; *Koskinen and Mälkki*, 1993] resulting in a weaker, less well defined potential drop that accelerate electrons, but not ions.

Although the field-aligned current for the event study of the previous section is very likely to be a driver of field-aligned acceleration in the auroral region, there are at least two indications that it is not the only driver that is present. The first indication from FAST (figure 4) is the

presence of an energized earthward streaming electron population at the most poleward edge of the auroral region before the satellite passes through the primary current region. Another indication is that FAST observed earthward streaming electrons after it passed into the return current region at lower latitudes. At the same time Polar data shows O^+ ions streaming tailward in the return current region (figure 7). In the return current region it would be expected that the field-aligned potential should reverse itself and accelerate electrons tailward and ions earthward [*Carlson et al.*, 1998b], which does not seem to be the case in the event study. We now consider other magnetotail drivers that can account for these observations.

4.2 PSBL Beams/Quasi-Static Potential Drops

In the June 9, 1997 event study discussed in section 3, Polar observed high-energy earthward streaming ion beams in the PSBL that originate from the magnetotail. Such beams have been proposed as causing electrostatic shocks and parallel potential drops in the auroral zone that ultimately accelerate auroral particles [*Kan*, 1975; *Kan and Akasofu*, 1976; *Lui et al.*, 1977; *Frank et al.*, 1981; *Lyons and Evans*, 1984]. The basic mechanism involved is the earthward streaming ion beams flowing towards the Earth represent an energy anisotropy and this anisotropy causes the plasma sheet ions and electrons mirror at different altitudes [*Alfvén and Fälthammer*, 1963; *Persson,* 1963; *Whipple*, 1977]. For the case of an ion beam streaming from the magnetotail towards the Earth, the ions mirror at an altitude lower than the electrons, setting up a potential drop oriented such that a tailward-directed parallel electric field forms. This parallel electric field then accelerates electrons earthward and ions tailward. For typical PSBL ion beam energies the potential drop that results in the auroral zone can be estimated using the following formula [*Serizawa and Sato*, 1984]:

$$q\Delta\phi \approx \frac{W_{i\parallel}}{1+T_i/T_e}$$

where $W_{i||}$ represents the ion beam kinetic energy, T_i is the ion temperature and T_e is the electron temperature. In the event study two PSBL beams were discussed in figure 8 and figure 9. The ion beam kinetic energy was about 3.7 keV in one case and about 40 keV in the other case. Using an estimated ion to electron temperature ratio of $T_i/T_e \sim 5$ [e.g., *Frank*, 1985] gives a potential drop of $\Delta\phi \sim 620$ V and $\Delta\phi \sim 5$ kV, respectively for the two different beam energies. Numerical simulations showed that this value can be reduced up to 10% by wave-particle interactions [*Schriver*, 1999]. These values for the potential drop that would form in the auroral zone due the PSBL beam driver are consistent with the 1 kV value inferred from the precipitating electrons and upwelling ions observed by FAST and Polar.

Numerical simulations have been used to examine the structure of the potential drop that forms in this situation for the case of the more energetic PSBL ion beam (40 keV). The electrostatic particle-in-cell (PIC) code includes the magnetic mirror force, cold ionospheric plasma, and warm plasma that can be injected from the magnetotail plasma sheet [*Schriver*, 1999]. The simulation system is one-dimensional and aligned along the ambient magnetic field. Using a variable grid scheme with about 93000 grids, a system length of about 20000 km is achieved. The low altitude end of the simulation system is set at 1000 km, and a cold ionospheric plasma is loaded in hydrostatic equilibrium. At the high altitude end of the system (~ 21000 km altitude) a population of relatively warm tenuous plasma from the magnetotail is included with an ion beam injected towards the Earth from the magnetotail. As discussed in section 3, the beam density relative to the background density is difficult to determine, and for the run here the densities are taken to be equal ($n_{\text{beam}} = n_{\text{background}}$). Figure 11 shows ion phase space at the beginning of the simulation run on the left and at the end of the simulation run at $\omega_{pe}t = 225000$ on the right. The panels show velocity (normalized to the warm plasma electron

thermal speed) versus altitude in the simulation system with red representing higher phase space density and blue lower phase space density. In each panel, since the horizontal axis is altitude, the Earth is to the left and the magnetotail plasma sheet to the right. The black curve shows the electric potential across the system in kV. As in previous simulation runs [e.g. *Schriver*, 1999], the PSBL ions and electrons are started with the same earthward drift such that initially there is no net current in the plasma. As the ions and electrons move earthward, both are affected by the mirror force, however, the streaming ions can penetrate to lower altitudes than the electrons thereby setting up a potential drop of about 2.5 kV across the system above about 6000 km altitude (right panel of figure 11). There is a slight potential increase (~ 0.5 kV) that occurs below about 6000 km, which is a transient effect that moves across the system with the beam as it moves closer to the Earth. This transient effect diminishes as the beam reaches its mirror point. Previous simulations with a shorter system also produced this transient potential increase which eventually vanished [*Schriver*, 1999]. Once the main potential drop above 6000 km forms it remains relatively static over the course of the run (several seconds in real time for this run) as long as the beam is continuously injected. If the beam driver is no longer injected into the system, the potential drop relaxes and eventually vanishes as the magnetotail ions and electrons converge to the same mirror point by the potential [*Schriver*, 1999]. The magnitude of the potential drop in the simulation is about half that estimated from the analytical formula above and is reduced by wave-particle interactions and thermal dissipation [*Schriver*, 1999].

The quasi-static potential drop that forms due to the anisotropy mirror mechanism corresponds to an electric field pointing away from the Earth, which can accelerate electrons towards the Earth and ions away from the Earth. Examples of accelerated distributions in the simulation are shown in figure 12, with electrons at low altitude on the left and ionospheric ions

at higher altitudes on the right. The left panel in figure 12 shows that for low altitude electrons a high-energy tail forms on the distribution function in the earthward direction (extension in negative velocity compared to the initial distribution function). The (ionospheric) ions at higher altitudes shown on the right panel of figure 12 have also been accelerated to form a beam-like distribution compared to the initial distribution function. Wave-particle interactions have modified both distribution functions. Any beam-like features of the electron distribution have been smeared by electron plasma oscillations, while a lower frequency ion-ion acoustic type wave has thermalized the ions somewhat giving the distribution a spread towards more negative velocities [*Bergmann and Lotko*, 1986; *Dusenbery and Martin*, 1987]. The accelerated distributions formed in the simulation are in qualitative agreement with the precipitating electron distribution observed by FAST at lower altitudes (figure 5) and the upgoing ion distribution observed at Polar at high altitudes (left panel of figure 8).

4.3 Poynting Flux/Kinetic Alfvén Waves

The third magnetotail driver of auroral acceleration we consider is Poynting flux propagating towards the Earth [*Wygant et al.*, 2000; *Keiling et al.*, 2001]. This Poynting flux is in the form of Alfvén waves generated at some location down the magnetotail (at least tailward of the Polar satellite) which propagate essentially along field lines in the earthward direction. How these magnetospheric Alfvén waves are generated in the first place is an interesting and unresolved problem in its own right, but is beyond the scope of this paper. The general mechanism is that as these magnetospheric Alfvén waves get closer to the Earth finite electron inertia effects can cause a parallel electric field component to develop that ultimately causes field-aligned electron acceleration in the auroral zone [*Hasegawa*, 1976; *Mallinckrodt and Carlson*, 1978; *Goertz and Boswell*, 1979]. Various models describing the properties of kinetic

Alfvén waves have been developed for conditions found in the near-Earth auroral region [e.g., *Lysak*, 1990, 1991].

Particles can be accelerated by kinetic Alfvén waves because they have a relatively low frequency ($\leq$ 1 Hz), and on electron time scales the parallel electric field appears to be quasi-static. Numerical models based on this basic premise have shown that electron acceleration can occur in the presence of kinetic Alfvén waves [*Temerin et al.*, 1986; *Kletzing*, 1994; *Thompson and Lysak*, 1996]. These models indicate that in order for these waves to induce electron acceleration, their scale transverse to the geomagnetic field must be comparable to the electron skin depth. Thus the kinetic Alfvén waves have very long wavelengths (of the order of several thousand kilometers) in the field-aligned direction and relatively short wavelengths in the perpendicular direction (< 10 km). For such a situation, *Temerin et al.* [1986] found that test electrons could be accelerated up to energies of several keV for Alfvén waves with an amplitude of about 10 mV/m. *Thompson and Lysak* [1996], also using a test particle approach, found that for an Alfvén wave with an amplitude of 0.6 mV/m (potential of 3 kV) and a static parallel potential drop of 6 kV, electrons could be accelerated to energies of several keV due to Landau resonance and the static potential drop.

From the Polar observations the amplitude of the transverse component of the fluctuating electric field is estimated to be about 20 mV/m (see figure 7). The parallel component would then be about 100 times less than this [*Temerin et al.*, 1986] or about 0.2 mV/m. From the Polar satellite trajectory it is estimated that the satellite moves about 500 km in the field-aligned direction. Based on these very rough estimates, the parallel potential drop due to the kinetic Alfvén waves at the location of Polar would be about 100 V. The parallel electric field component, however, probably increases closer to the Earth due to field convergence and thus a

larger parallel potential drop could be present in the auroral zone below Polar. As shown by *Thompson and Lysak* [1996], if kinetic Alfvén waves are present along with a static potential drop formed either by field-aligned currents or the PSBL beams as discussed in the previous sections, electrons could easily be accelerated to the keV energies observed by the FAST satellite.

The previous studies of the effects of kinetic Alfvén waves in the auroral zone have been for electrons. How kinetic Alfvén waves might affect ions is not clear. For an electron, a wave with a frequency of 1 Hz would appear as a quasi-static wave and acceleration might occur due to the parallel electric field component. Thus for a kinetic Alfvén wave with properties that vary with altitude, coherent acceleration is possible. For the more massive ions, however, such a wave would appear to be fluctuating and very little acceleration would probably occur. Unless the frequency is much lower ($<<$ 1 Hz), it is difficult to see how a kinetic Alfvén wave with properties discussed above would lead to coherent ion acceleration. This is important since upwelling ions are common in the auroral zone and were discussed in the event study of the previous section. Thus although precipitating electrons could be accelerated by kinetic Alfvén waves, tailward streaming ion beams are probably caused by a parallel potential drop driven either by field-aligned currents or the PSBL beam already discussed.

5. Conjunction Event Survey

We now consider all of the conjunction events we have examined so far in terms of magnetotail drivers. The results are summarized in Table 1. These events include the cases in which all of the relevant particle and field data from both satellites (FAST and Polar) have been examined. The results in Table 1 are broken down by event in the first column, field-aligned acceleration in the next three columns, and the presence of the possible magnetotail drivers in the

last three columns. The field-aligned acceleration columns provide the earthward electron streaming energy (at lower altitudes from FAST), upflowing ion beam (UFIB) streaming energy (if present), and upflowing electron (UFE) streaming energy (if present), both at higher altitudes from Polar. The magnetotail driver columns indicate the presence of Alfvén waves, a PSBL ion beam (earthward flow), and a field-aligned current (FAC), all as detected by Polar at high altitudes.

A total of seven events have been analyzed, as shown in Table 1. In all cases, the electron precipitation occurred in regions of field-aligned current (second and last columns). Two events had both upflowing ions and electrons (June 9 and August 3). The June 9 event was discussed in section 3. In both cases the electron precipitation energy was relatively high and both Poynting flux and PSBL (ion) beam drivers were present. One case (July 20) had Alfvén waves, but no PSBL beam. Four cases had relatively weak electron precipitation and the only discernable driver was a field-aligned current. In all of the cases, FAST observed small-scale structures embedded in the larger scale field-aligned current sheets and the field-aligned energized electrons were usually bursty, similar to the events shown in figures 3 and 4. Also, similar to the events discussed in figures 3 and 4, correspondence between the fine-scale current structures and the electron bursts occurred some of the time, but not always.

Although more events need to be examined, some general patterns appear in the results shown in Table 1 that are consistent with the physics of auroral drivers discussed in the previous section. When the Alfvén waves and field-aligned currents were present without the PSBL beam there is no upflowing ion beam although there were indications of upwelling field-aligned electrons. This is consistent with a kinetic Alfvén wave that can accelerate electrons in the field-aligned direction, but cannot accelerate ions. Also, the parallel potential drop formed by the

field-aligned current apparently was not strong enough or quasi-static on ion time scales and thus also did not accelerate ions tailward. On the other hand, upflowing ion beams were present when a PSBL ion beam driver was also present, which is consistent with the formation of a large-scale potential drop that could accelerate ions away from the Earth. Cases in which only the field-aligned current was present (no Alfvén waves or PSBL beams) suggest that a weak double layer existed in the auroral zone that could accelerate electrons earthward but did not have a strong effect on the ions (forming upwelling distributions).

It is interesting to note that the events with energetic precipitation along with both outflowing ions and electrons (June 9 and August 3) occurred during times of increased magnetic activity. The June 9 case (as already mentioned) occurred very close to the peak of a magnetic storm (Dst = -84 nT), while the August 3 case occurred at the beginning (Dst = -40 nT) of a storm that peaked about 2 to 3 hours later. The July 20 event (Alfvén waves and field-aligned currents) occurred during moderate activity (Dst = -18), although a substorm may have been active at that time. All of the other events in Table 1 were during relatively quiet times.

6. Conclusions

FAST/Polar conjunction events were used in a study to identify drivers of field-aligned auroral acceleration. The physics of the possible magnetotail drivers and auroral accelerators has been considered to help understand and interpret the satellite data. A total of 7 events have been examined in detail for which FAST observed field-aligned electrons streaming earthward and Polar was in near-conjunction high above the FAST satellite location. From the events examined thus far it appears that three magnetotail drivers were present that led to auroral acceleration. Based on the various combinations of accelerated distributions observed during different activity levels, the three driver/accelerators are listed below along with their characteristics:

(1) Field-Aligned Current/Quasi-static Potential Drop - during quiet times results in earthward electron acceleration, but no tailward ion acceleration. Upwelling electrons are associated with the return current region.

(2) PSBL Beam/Quasi-static Potential Drop - during active times can accelerate electrons earthward and ions tailward.

(3) Poynting Flux/Kinetic Alfvén Waves - during active times can accelerate electrons towards the Earth. Does not correlate with tailward ion flow, but might be associated with tailward streaming electrons.

These three driver/accelerators can occur all at the same time or separately, with their presence depending mainly on magnetic activity level. The field-aligned current was always present, however, during more active times the Alfvén waves and PSBL beam were also present, and during one moderately active event only the Alfvén waves was detected (no PSBL beam). During quiet times only the field-aligned current was present. Since only seven events have been examined thus far, these results must be considered as preliminary. A simulation study that includes field-aligned currents and kinetic Alfvén waves is presently underway to examine the effects or these drivers on both electrons and ions for various conditions. Also additional conjunction events are being examined.

Despite the preliminary nature of the findings thus far, the results follow a pattern consistent with the physics of the different magnetotail drivers. For example, when kinetic Alfvén waves were present, electrons were accelerated earthward as expected for a slowly varying (on electron time scales) parallel electric field. The formation of upwelling ion beams, however, requires the presence of a strong quasi-static parallel electric field, which can be supported by strong field-aligned currents or a PSBL beam. This is consistent with observations

that indicate the presence of upwelling ions when the field-aligned current is strong and/or when a PSBL beam is present. When neither the Alfvén wave driver nor the PSBL beam driver were present, the field-aligned current, which was relatively weak in those cases, resulted in relatively low energy electron precipitation and no upwelling beam populations. It is interesting to note that these accelerators taken either together or separately can account for all of the forms of field-aligned electron and ion acceleration found in the primary current region in this study.

One of the features found in the electrons observed by FAST is the bursty nature of the field-aligned acceleration (in latitude), along with small-scale structures in the current embedded in the overall large-scale field-aligned current sheets. This can be seen in both figures 3 and 4 and was found in all of the seven events discussed in Table 1. A close look at the electron peaks at 0^{o} pitch angle (panel two of figures 3 and 4) and the fine scale structures in the magnetic field (bottom panel of figures 3 and 4) show that there is correspondence some of the time, but not all of the time. It is not clear what causes the structure in electron acceleration or the magnetic field. One possibility is that density perturbations in the auroral zone (above FAST) that lead to the formation of strong potential drops in the overall field-aligned current sheet are structured and this leads to the structured electron acceleration. Another possibility is that the fluctuating nature of the kinetic Alfvén waves leads to the structured electron acceleration akin to the flickering aurora discussed by *Temerin et al.* [1986]. It is also possible that the Alfvén waves and/or PSBL ion beams are structured in latitude from their magnetospheric source region downtail. We are in the process of examining the origin of these structures by looking more closely at the satellite data and by using new large-scale multi-dimensional auroral simulations.

The findings here correspond mainly to the primary current region (field-aligned current directed away from the Earth) where accelerated electrons have been observed to stream towards

the Earth. The study has not considered in detail the return current region (field-aligned current directed towards the Earth), in which it is expected that everything should essentially be reversed such that the quasi-static electric field points towards the Earth, and field-aligned ions stream earthward and electrons stream tailward [*Marklund et al.*, 1994; 1997; *Carlson et al.*, 1998b]. In the return current region the dynamics are quite different from those of the primary current region since the drivers may originate from the ionosphere (rather than the magnetosphere). In the return current region, current-driven double layers in a cold ionospheric plasma might play a prominent role in the acceleration process [*Newman et al.*, 2001], or wave-particle interactions, along with the mirror force, could be important [*Jasperse and Grossbard*, 2000].

Although we have identified three primary drivers of field-aligned electron acceleration in the primary current region, it remains to be determined how and where the magnetotail drivers originate. Both the Poynting flux and the PSBL beams, since they tend to occur in the plasma sheet boundary layer, may indicate a relation to magnetic reconnection in the magnetotail. For example, a forced one-dimensional current sheet modeled using a hybrid simulation has been shown to radiate incompressible Alfvén waves [*Pritchett and Coroniti,* 1993]. Another possibility is that shear Alfvén waves are excited at the inner magnetotail boundary between cold and hot plasmas [*Lee et al.*, 2000]. The formation of the energetic earthward streaming ion beams in the PSBL is not well understood, with reconnection and non-adiabatic particle motion being possibilities [*Lyons and Speiser,* 1982; *Schindler and Birn,* 1987; *Ashour-Abdalla et al.*, 1991]. The appearance of the energetic PSBL beams during times of high magnetic activity might be related to a large parallel electric field that can form for highly disturbed magnetospheric conditions [*Siscoe et al.*, 2001]. Another unresolved problem is how these

drivers are reconciled with the global current system. These important global issues that must be considered to ultimately understand the causes of the aurora.

Acknowledgments. The authors would like to thank E. Dors, J. Dorelli and M. El-Alaoui for useful comments and discussions related to this project. We also wish to thank C.T. Russell for the use of Polar magnetic field data, F.S. Mozer for the use of Polar electric field data and G. Parks for the UVI data. This research was funded by NASA Guest Investigator Grant NAG5-10473, NASA Geospace Sciences Grant NAG5-11989, NASA ISTP Grant NAG5-6689 and LANL-IGPP Grant 01-1115. Computing resources were provided by the NSF National Partnership for Advanced Computing Infrastructure (NPACI).

Conjunction	**Field Aligned Acceleration**			**Magnetotail Driver**		
Date/Time (UT)	Electrons	UFIB	UFE	Alfvén Waves	PSBL Beam	FAC
Jun 9, 1997 04:32	~ 1 keV	~ 1 keV	~ 1 keV	X	X	X
Jul 20, 1997 16:24	.1-1. keV		.1-1. keV	X		X
Jul 22, 1997 15:21	.1-1. keV					X
Jul 24, 1997 20:40	.1-1. keV					X
Jul 26, 1997 14:25	.1-1. keV					X
Jul 26, 1997 16:45	.1-1. keV					X
Aug 3, 1997 17:46	~ 1 keV	~ 0.1 keV	~ 0.1 keV	X	X	X

Table 1. Presented here is a list of FAST/Polar auroral conjunction events. Electron field-aligned acceleration measured by the FAST satellite is earthward directed in all cases. UFIB stands for upflowing ion beams (away from the Earth) and UFE is for upflowing electrons, both as measured by Polar. Alfvén waves and PSBL beams are earthward directed from the magnetotail, and FAC is field-aligned current, usually in the tailward directed sense. All magnetotail drivers are observed by the Polar satellite.

References

Alfvén, H., and C.G. Fälthammer, *Cosmical Electrodynamics*, Clarendon, Oxford, 1963.

Ashour-Abdalla, M., J. Berchem, J. Büchner, and L.M. Zelenyi, Large and small scale structures in the plasma sheet: A signature of chaotic motion and resonance orbits, *Geophys. Res. Lett.*, *18*, 1603, 1991.

Baumjohann, W., G. Paschmann, and C.A. Cattell, Average plasma properties in the central plasma sheet, *J. Geophys. Res.*, *94*, 6597, 1989.

Bergmann, R., and W. Lotko, Transition to unstable ion flow in parallel electric fields, *J. Geophys. Res.*, *91*, 7033, 1986.

Blake, J.B., J.F. Fennell, L.M. Friesen, B.M. Johnson, W.A. Kolasinski, D.J. Mabry, J.V. Osborn, S.H. Penzin, E.R. Schnauss, H.E. Spence, D.N. Baker, R. Belian, T.A. Fritz, W. Ford, D. Laubscher, R. Stiglich, R.A. Baraze, M.F. Hilsenrath, W.L. Imhof, J.R. Kilner, J. Mobilia, D.H. Voss, A. Korth, M. Gull, K. Fisher, M. Grande, and H. Dall, CEPPAD (Comprehensive Energetic Particle and Pitch Angle Distribution) on Polar, *Space Sci. Rev.*, *71*, 563, 1995.

Block, L.P., Potential double layers in the ionosphere, *Cosmic Electrodyn.*, *3*, 349, 1972.

Block, L.P., A double layer review, *Astrophys. Space Sci.*, *55*, 59, 1978.

Carlqvist, P., *Cosmic Electrodyn.*, *3*, 377, 1972.

Carlson, C.W., R.F. Pfaff, and J.G. Watzin, The Fast Auroral SnapshoT (FAST) mission, *Geophys. Res. Lett.*, *25*, 2013, 1998a.

Carlson, C.W., J.P. McFadden, R.E. Ergun, M. Temerin, W. Peria, F.S. Mozer, D.M. Klumpar, E.G. Shelley, W.K. Peterson, E. Moebius, R. Elphic, R. Strangeway, C. Catell, and R. Pfaff, FAST observations in the downward current region: Energetic upgoing electron beams, parallel potential drops, and ion heating, *Geophys. Res. Lett*, *25,* 2017, 1998b.

Chiu, Y.T., and J.M. Cornwall, Electrostatic model of a quiet auroral arc, *J. Geophys. Res.*, *85,* 543, 1980.

Chiu, Y.T., J.M. Cornwall, and M. Schulz, Effects of auroral-particle anisotropies and mirror forces on high-latitude electric fields, *Physics of Auroral Arc Formation,* edited by S.-I., Akasofu and J.R. Kan, *Geophys. Mono. Ser., 25*, 234, American Geophysical Union, Washington, D.C., 1981.

Christensen, A.B., L.R. Lyons, J.H. Hecht, G.G. Sivjee, R.R. Meier, and D.G. Strickland, Magnetic field-aligned electric field acceleration and characteristics of the optical aurora, *J. Geophys. Res.*, *92,* 6163, 1987.

DeCoster, R.J., and L.A. Frank, Observations pertaining to the dynamics of the plasma sheet, *J. Geophys. Res.*, *84,* 5099, 1979.

Dusenbery, P.B., and R.F. Martin, Jr., Generation of broadband turbulence by accelerated auroral ions, 1. Parallel propagation, *J. Geophys. Res.*, *92*, 3261, 1987.

Eastman, T.E., L.A. Frank, W.K. Peterson, and W. Lennartsson, The plasma sheet boundary layer, *J. Geophys. Res.*, *89,* 1553, 1984.

Elphic, R.C., J.W. Bonnell, R.J. Strangeway, L. Kepko, R.E. Ergun, J.P. McFadden, C.W. Carlson, W. Peria, C.A. Cattell, D. Klumpar, E. Shelley, W. Peterson, E. Moebius, L. Kistler, and R. Pfaff, *Geophys. Res. Lett*, *25,* 2033, 1998.

Ergun, R.E., C.W. Carlson, J.P. McFadden, and F.S. Mozer, Parallel electric fields in discrete arcs, *EOS Trans., 81*, F1026, 2000.

Eriksson, A.I., and R. Boström, Are weak double layers important for auroral particle acceleration?, in *Auroral Plasma Dynamics, Geophys. Mono., 80,* edited by R.L. Lysak, pp. 105, American Geophysical Union, Washington, D.C., 1993.

Evans, D.S., Precipitating electron fluxes formed by a magnetic field aligned potential difference, *J. Geophys. Res., 79,* 2853, 1974.

Frank, L.A., Plasmas in the Earth's magnetotail, *Space Sci. Rev., 42*, 211, 1985.

Frank, L.A., and K.L. Ackerson, Observations of charged particle precipitation into the auroral zone, *J. Geophys. Res., 76*, 3612, 1971.

Frank, L.A., K.L. Ackerson, and R.P. Lepping, On hot tenuous plasmas, fireballs, and boundary layers in the Earth's magnetotail, *J. Geophys. Res., 81,* 5859, 1976.

Frank, L.A., R.L. McPherron, R.J. DeCoster, B.G. Burek, K.L., Ackerson, and C.T. Russell, Field aligned currents in the Earth's magnetotail, *J. Geophys. Res., 86,* 687, 1981.

Ghielmetti, A.G., R.G. Johnson, R.D. Sharp, and E.G. Shelley, The latitudinal, diurnal, and altitudinal distributions of upward flowing energetic ions of ionospheric origin, *Geophys. Res. Lett., 5,* 59, 1978.

Goertz, C.K., and G. Joyce, Numerical simulation of the plasma double layer, *Astrophys. Space Sci., 32,* 165, 1975.

Goertz, C.K., and R.W. Boswell, Magnetosphere-ionosphere coupling, *J. Geophys. Res., 84,* 7239, 1979.

Gorney, D.J., J.A. Clarke, D. Croley, J. Fennel, J. Luhmann, and P. Mizera, The distribution of ion beams and conics below 8000 km, *J. Geophys. Res., 86,* 83, 1981.

Haerendel, G., Field-aligned currents in the Earth's magnetosphere, *Geophys. Mono. Ser., 58,* 539, American Geophysical Union, Washington, D.C., 1990.

Harvey, P., F.S. Mozer, D. Pankow, J. Wygant, N.C. Maynard, H. Singer, W. Sullivan, P.B. Anderson, R. Pfaff, T. Aggson, A. Pedersen, C.G. Fälthammer, and P. Tanskannen, The electric field instrument on the Polar satellite, *Space Sci. Rev., 71,* 583, 1995.

Hasegawa, A., Particle acceleration by MHD surface wave and formation of aurora, *J. Geophys. Res., 81,* 5083, 1976

Hoffmann, R.A., and D.S. Evans, Field-aligned electron bursts at high latitude observed by Ogo 4, *J. Geophys. Res., 73,* 6201, 1968.

Hones, E.W., Jr., J.R. Asbridge, S.J. Bame, M.D. Montgomery, S. Singer, and S.-I. Akasofu, Measurements of magnetotail plasma flow make with Vela 4B, *J. Geophys. Res., 77,* 5503, 1972.

Hultqvist, B., H. Borg, W. Reidler, and P. Chistopherson, Observations of a magnetic field-aligned anisotropy for 1 and 6 keV positive ions in the upper ionosphere, *Planet. Space Sci., 19,* 279, 1971.

Iijima, T., and T.A. Potemra, The amplitude distribution of field-aligned currents at northern high latitudes observed by TRIAD, *J. Geophys. Res., 81,* 2165, 1976.

Jasperse, J.R. and N.J. Grossbard, The Alfvén-Fälthammer formula for the parallel E field and its analogue in downward auroral-current regions, *IEEE Trans. Plasma Sci.,* Dec., 2000.

Kan, J.R., Energization of auroral electrons by electrostatic shock waves, *J. Geophys. Res., 80,* 2089, 1975.

Kan, J.R., and S.-I. Akasofu, Energy source & mechanisms for accelerating the electrons and driving the field-aligned currents of the discrete auroral arc, *J. Geophys. Res.*, *81,* 5123, 1976.

Kennel, C.F., Consequences of a magnetospheric plasma, *Rev. Geophys., 7*, 379, 1969.

Kennel, C., and H. Petschek, Limit on stable trapped particle fluxes, *J. Geophys. Res.*, *71,* 1, 1966.

Keiling, A., J.R. Wygant, C. Cattell, M. Johnson, M. Temerin, F.S. Mozer, C.A. Kletzing, J. Scudder, and C.T. Russell, Properties of large electric fields in the plasma sheet at 4-7 RE measured with Polar, *J. Geophys. Res.*, *106*, 5779, 2001.

Kletzing, C.A., Electron acceleration by kinetic Alfvén waves, *J. Geophys. Res.*, *99,* 11095, 1994.

Kletzing, C.A., and J.D. Scudder, Auroral-plasma sheet electron anisotropy, *Geophys. Res. Lett.*, *26,* 971, 1999.

Kletzing, C.A., and R.B. Torbert, Electron time dispersion, *J. Geophys. Res.*, *99,* 2159, 1994.

Knight, S., Parallel electric fields, *Planet. Space Sci., 21,* 741, 1973.

Koskinen, H.E.J., and A.M. Mälkki, Auroral weak double layers: A critical assessment, in *Auroral Plasma Dynamics, Geophys. Mono., 80,* edited by R.L. Lysak, pp. 97, American Geophysical Union, Washington, D.C., 1993.

Lee, D.H., R.L. Lysak, and Y. Song, Generation of field-aligned currents in the near-Earth magnetotail, *EOS (abstract), 81*, F1051, 2000.

Lemaire, J., and M. Scherer, Ionosphere-plasmasheet field-aligned currents and parallel electric fields, *Planet. Space Sci., 22,* 1485, 1974.

Lui, A.T.Y., E.W. Hones, Jr., F. Yasuhara, S.-I. Akasofu, and S.J. Bame, Magnetotail plasma flow during plasma sheet expansions: Vela 5 and 6 and IMP 6 observations, *J. Geophys. Res., 82,* 1235, 1977.

Lui, A.T.Y., T.E. Eastman, D.J. Williams, and L.A. Frank, Observation of ion streaming during substorms, *J. Geophys. Res., 88,* 8853, 1983.

Lyons, L.R., and D.S. Evans, An association between discrete auroral and energetic particle boundaries, *J. Geophys. Res., 89,* 2395, 1984.

Lyons, L.R., and T.W. Speiser, Evidence for current sheet acceleration in the geomagnetic tail, *J. Geophys. Res., 87,* 2276, 1982.

Lyons, L.R., T. Nagai, G.T. Blanchard, J.C. Samson, T. Yamamoto, T. Mukai, A. Nishida, and S. Kokubun, Association between Geotail plasma flows and auroral poleward boundary, *J. Geophys. Res., 104,* 4485, 1999.

Lysak, R.L., Auroral electrodynamics with current and voltage generators, *J. Geophys. Res., 90,* 4178, 1985.

Lysak, R.L., Electrodynamic coupling of the magnetosphere and ionosphere, *Space Sci. Rev.*, 52, 33, 1990.

Lysak, R.L., Feedback instability of the ionospheric resonant cavity, *J. Geophys. Res., 96,* 1553, 1991.

Lysak, R.L., The relationship between electrostatic shocks and kinetic Alfvén waves, *Geophys. Res. Lett., 25,* 2089, 1998.

Mallinckrodt, A.J., and C.W. Carlson, Relations between transverse electric fields and field-aligned currents, *J. Geophys. Res., 83,* 1426, 1978.

Marklund, G., L. Blomberg, C.G. Fälthammer, and P.-A. Lindqvist, On intense diverging electric fields associated with black aurora, *Geophys. Res. Lett.*, *21,* 1859, 1994.

Marklund, G., T. Karlsson, and J. Clemmons, On low-altitude particle acceleration and intense electric fields and their relationship to black aurora, *J. Geophys. Res.*, *102*, 1997.

McIlwain, C.E., Direct measurements of particles producing visible auroras, *J. Geophys. Res.*, *65*, 73, 1960.

Möbius, E., F.M. Ipavich, M. Scholer, G. Gloeckler, D. Hovestadt, and B. Klecker, Observation of nonthermal ion layer at the plasma sheet boundary during substorm recovery, *J. Geophys. Res.*, *85*, 5143, 1980.

Mozer, F.S. C. Carlson, M. Hudson, R. Torbert, B. Parady, J. Yatteau, and M. Kelley, Observations of paired electrostatic shocks in the polar magnetosphere, *Phys. Rev. Lett., 38*, 292, 1977.

Newman, D.L., M.V. Goldman, R.E. Ergun, and A. Mangeney, Formation of double layers and electron holes in a current-driven space plasma, *Phys. Rev. Lett., 87*, 2555001-1, 2001.

Persson, H., Electric field along a magnetic line of force in a low density plasma, *Phys. Fluids 6*, 1756, 1963.

Pritchett, P.L., and F.V Coroniti, A radiating one dimensional current sheet configuration, *J. Geophys. Res.*, *98,* 15355, 1993.

Rees, M.H., and D. Luckey, Auroral electron energy derived from ratio of spectroscopic emissions, 1. Model computations, *J. Geophys. Res.*, *79,* 5181, 1974.

Reiff, P.H., H.L. Collin, E.G. Shelley, J.L. Burch, and J.D. Winningham, Heating of upflowing ionospheric ions on auroral field lines, *Ion Acceleration in the Magnetosphere and*

Ionosphere, Geophys. Mono. Ser., vol. 38, edited by T. Chang, pp. 83, AGU, Washington D.C., 1986.

Reiff, P.H., H.L. Collin, J.D. Craven, J.L. Burch, J.D. Winningham, E.G. Shelley, L.A. Frank, and M.A. Friedman, Determination of auroral electrostatic potentials using high and low altitude particle distributions, *J. Geophys. Res.*, *93,* 7441, 1988.

Russell, C., R.C. Snare, J.D. Means, D. Pierce, D. Dearborn, M. Larson, G. Barr, and G. Le, The GGS/Polar magnetic fields investigation, *Space Sci. Rev., 71,* 563, 1995.

Schindler, K., and J. Birn, On the generation of field-aligned plasma flow at the boundary of the plasma sheet, *J. Geophys. Res.*, *92,* 95, 1987.

Schriver, D., Particle simulation of the auroral zone showing parallel electric fields, waves and plasma acceleration, *J. Geophys. Res.*, *104,* 14655, 1999.

Schriver, D., Simulating an inhomogeneous plasma system: Variable grids and boundary conditions, *Proceedings of the 6'th International School of Space Simulations (ISSS-6),* Springer-Verlag Publishers, in press, 2002.

Schriver, D., M. Ashour-Abdalla, R. Treumann, M. Nakamura, and L.M. Kistler, The lobe to plasma sheet boundary layer transition: Theory and observations, *Geophys. Res. Lett., 17,* 2027, 1990.

Scudder, J.D., F. Hunsacker, G. Miller, J. Lobell, T. Zawistowski, K. Ogilvie, J. Keller, D. Chornay, F. Herrero, R. Fitzenreiter, D. Fairfield, J. Needell, D. Bodet, J. Googins, C. Kletzing, R. Torbert, J. Vandiver, R. Bentley, W. Fillius, C. McIlwain, E. Whipple, and A. Korth, Hydra - A 3-dimensional electron and ion hot plasma instrument for the Polar spacecraft of the GGS mission, *Space Sci. Rev., 71,* 459, 1995.

Serizawa, Y., and T. Sato, Generation of large scale potential difference by currentless plasma jets along the mirror field, *Geophys. Res. Lett., 11,* 595, 1984.

Shelley, E.G., R.D. Sharp, and R.G. Johnson, Satellite observations of an ionospheric acceleration mechanism, *Geophys. Res. Lett., 3,* 654, 1976.

Siscoe, G.L., G.M. Erickson, B.U.O Sonnerup, N.C. Maynard, K.D. Siebert, D.R. Weimer, and W.W. White, Global role of $E_{||}$ in magnetopause reconnection: An explicit demonstration, *J. Geophys. Res., 106,* 13015, 2001.

Stenbaek-Nielsen, H.C., T.J. Hallinan, D.L. Osborne, J. Kimball, C. Chaston, J. McFadden, G. Delory, M. Temerin, and C.W. Carlson, Aircraft observations conjugate to FAST: Auroral arc thicknesses, *Geophys. Res. Lett, 25,* 2033, 1998.

Swift, D.W., On the formation of auroral arcs and acceleration of auroral electrons, *J. Geophys. Res., 80,* 2096, 1975.

Takahashi, K., and E.W. Hones, Jr., ISEE 1 and 2 observations of ion distributions at the plasma sheet-tail lobe boundary, *J. Geophys. Res., 93,* 8558, 1988.

Temerin, M.A., J. McFadden, M. Boehm, C.W. Carlson, and W. Lotko, Production of flickering aurora and field-aligned electron flux by electromagnetic ion cyclotron waves, *J. Geophys. Res., 91,* 5769, 1986.

Thompson, B.J., and R.L. Lysak, Electron acceleration by inertial Alfvén waves, *J. Geophys. Res., 101,* 5359, 1996.

Torr, M.R., D.G. Torr, M. Zukic, R.B. Johnson, J. Ajello, P. Banks, K. Clarke, K. Cole, C. Keffer, G. Parks, B. Tsurutani, and J. Spann, A far ultraviolet imager for the international solar-terrestrial physics mission, *Space Sci. Rev., 71,* 329, 1995.

Tsyganenko, N.A., A magnetospheric magnetic field model with a warped tail current sheet, *Planet. Space Sci., 37*, 5, 1989.

Tsyganenko, N.A., and D.P. Stern, Modeling the global magnetic field of the large-scale Birkeland current systems, *J. Geophys. Res., 101*, 27187, 1996.

Vasyliunas, V.M., Fundamentals of current description, *Magnetospheric Currents, Geophys. Mono., 28,* edited by T.A. Potemra, American Geophysical Union, pg. 63, 1983.

Whipple, E.C., The signature of parallel electric fields in a collisionless plasma, *J. Geophys. Res., 82,* 1525, 1977.

Wygant, J. R., A. Keiling, C.A. Cattell, M. Johnson, R.L. Lysak, M. Temerin, F.S. Mozer, C.A. Kletzing, J. D. Scudder. W. Peterson, C. T. Russell, G. Parks, M. Brittnacher, G. Germany, and J. Spann, Polar spacecraft based comparisons of intense electric fields and Poynting flux near and within the plasma sheet-tail lobe boundary to UVI images: An energy source for the auroral, *J. Geophys. Res., 106,* 18675, 2000.

Figure Captions

Figure 1. Projection of FAST and Polar satellite tracks onto the Earth's North Pole on June 9, 1997. The long red line is the track of FAST from about 04:15 UT to 04:40 UT. The shorter white (surrounded by blue) line in the bottom left quadrant shows Polar from about 04:00 UT to 05:00 UT. The green ovals show the nominal auroral zone and the yellow curve shows the nominal terminator. An auroral conjunction event occurs at about 04:32 UT, when the FAST (red) and Polar (white) paths cross. This plot was adapted from the website at http://teams.spasci.com/conjunctions.html, which was produced using software modified by Karl Heinz Trattner at Lockheed.

Figure 2. Schematic diagram showing the relative positions of the FAST and Polar satellites in the GSM *x-z* plane near conjunction. The Earth is at the lower left and the thin black lines show the mapping of auroral latitude magnetic field lines from the Earth towards the magnetotail. The thicker black line shows the approximate location of the most poleward last closed field line. Due the converging of the magnetic field and the satellite speeds, FAST moves through the auroral region much quicker than Polar.

Figure 3. Data from the FAST satellite during an auroral conjunction event on July 20, 1997. The top panel shows electron energy spectra (in eV); the middle panel shows electron pitch angle with 0^{o} corresponding to the earthward direction and 180^{o} away from the Earth; the bottom panel shows the magnetic field components (in nT) in the east-west direction (green e trace), the field-aligned direction (blue b trace) and the direction transverse to e and b (red o trace). Earthward directed electron flux events are evident between about 16:23 and 16:25

UT as a series of red bursts at 0° pitch angle in the second panel. The energies of these earthward directed bursts is between about 100 and 1000 eV as seen in the top panel.

Figure 4. FAST data is shown for the auroral conjunction event on June 9, 1997. The format is the same as figure 3 showing electron energy and pitch angle in the top two panels and the magnetic field in the bottom panel with the field-aligned component (b) in blue, the east-west component (e) in green and the component transverse to these two components (o) in red. For this event FAST, going from high to lower latitudes crosses from the polar cap into the auroral region at about 04:31:30 UT as evidenced by the sudden appearance of high energy electrons (top panel) and the change in the east-west magnetic deflection (green line, bottom panel). From 04:31:30 UT until about 04:32:45 UT, FAST passes through a region of net field-aligned current pointing tailward (labeled FAC-) consistent with a region 1 current on the dusk side. After 04:32:45 UT, FAST then goes through a gradual region of return current (labeled FAC+). Bursts of field-aligned energized electrons occur intermittently when FAST is in the auroral zone as seen by the (red) peaks in 0° pitch angle in the middle panel.

Figure 5. Electron distribution function taken for the conjunction event shown in the previous figure for June 9, 1997 at around 04:32 UT. Velocity space contours are shown with the perpendicular velocity being along the vertical axis in km/s and the parallel velocity along the horizontal axis (also in km/s). The contours are elongated in the positive parallel direction, which corresponds to the direction towards the Earth, indicating there is a net earthward flux of electrons. Such a feature appears as a peak in 0° pitch angle seen in the middle panel of figure 4.

Figure 6. Data from the MFE magnetic field instrument (courtesy of C. Russell) and from the EFI electric field instrument (courtesy of F. Mozer) on the Polar satellite are shown for the

time interval from 04:20 to 04:40 UT on June 9, 1997. On the top panel the B_x (blue line), B_y (red line), B_z (green line) magnetic field components in GSM coordinates are shown where the field is subtracted from the *Tsyganenko and Stern* [1996] field model. The bottom panel shows the E_z electric field component in GSE coordinates. When the Polar satellite crosses from the polar cap (open field lines) into the near-Earth plasma sheet at about 04:23 UT, there are large fluctuations in both the magnetic and electric fields associated with a large amplitude Alfvén wave (labeled AW above the top panel). After about 04:25 UT, dB_x (blue line) strongly decreases which indicates the satellite is passing through a region of field-aligned current directed tailward (FAC-) associated with a region 1 current. A modest increase in dB_x after about 04:28 UT implies the satellite is going through the return current region, which is directed earthward (labeled FAC+).

Figure 7. Polar particle data from the Hydra instrument is shown for the auroral conjunction event on June 9, 1997. The top two panels show electron data with the top panel the energy spectra (in eV) and the second panel the skew. The bottom two panels show the same quantities for ions. The skew is the difference in count rate between the field-aligned and the anti-field-aligned particles. It is normalized to the one sigma error and thus gives a sense of the net field-aligned flow either towards the Earth (yellow-red) or away from the Earth (green-blue). Ion flow away from the Earth is seen in the bottom panel as dark blue regions at about 1 keV from about 04:26 UT to 04:28 UT and again from about 04:31 UT to about 04:34 UT. At higher energies (> 10 keV) there are indications of an earthward ion flow (yellow) also seen in the bottom panel. Tailward directed electron flow can be seen as a darker blue region near 04:35 UT in the second panel.

Figure 8. Ion distribution functions from the Hydra instrument are shown at two different times at 04:32 UT on the left and 04:35 UT on the right for the June 9, 1997 event. Perpendicular velocity (to the ambient magnetic field) is along the vertical direction and parallel velocity is along the horizontal direction. The left panel shows ionospheric oxygen ions streaming tailward away from the Earth at about −100 km/s. The right panel shows a kidney bean shaped PSBL hydrogen ion beam of magnetotail origin at about 600 km/s streaming earthward.

Figure 9. Ion data from the CEPPAD instrument onboard Polar is shown at about 04:32 UT for the June 9, 1997 event. Count rate versus pitch angle is shown where 0° is towards the Earth and 180° is away from the Earth. Data in this figure is taken from the 35.4 keV energy channel. Peaks in the count rate occur when the pitch angle is field-aligned towards the Earth (0°), and minima tend to occur in the anti-earthward direction (180°). This trend is also present in other energy channels from about 15 keV to about 65 keV, with a peak in the 35 and 45 keV energy channels.

Figure 10. Data from the UVI instrument on the Polar satellite (courtesy of G. Parks) is shown for the June 9, 1997 conjunction event at 04:32 UT. Auroral enhancements can be seen between about 60° and 70° latitude. The FAST/Polar conjunction field is mapped to the point on the Earth indicated by the X, near about 70° latitude and 20 MLT.

Figure 11. Ion phase space snapshots at two different times are shown from an auroral simulation in which an ion beam is injected into the system. Velocity normalized to ion thermal velocity is shown versus position along the simulation system, which is along the terrestrial magnetic field. The horizontal axis has been normalized to kilometers and represents altitude above the Earth. The black line across the system shows the self-

consistently generated electrostatic potential in kilovolts. In each panel the Earth is to the left and the magnetotail is to the right. The initial condition at $t = 0$ is shown in the left panel and the PSBL warm ion beam can be seen flowing from right to left (toward the Earth). As time proceeds in the simulation, the ion beam mirrors at a lower altitude than the PSBL electrons, leading to a quasi-static ~ 2.5 kV potential drop across the system above 6000 km seen in the right panel which shows results near the end of the run. This potential drop corresponds to a parallel electric field pointing away from the Earth over an altitude range of several thousand kilometers.

Figure 12. Electron and ion distribution functions from the simulation run shown in the previous figure are presented. The electron distribution function on the left is shown at lower altitudes in the simulation system binned between 1000 km and 3500 km. The ion distribution on the right is shown for a spatial bin between 5000 km and 9000 km. In both panels the dotted line shows the initial distribution function for reference. For the low altitude electrons (left panel), a high-energy tail of particles streaming earthward (negative velocities) is created by the quasi-static parallel electric field that forms. The higher altitude ions (right panel) are accelerated away from the Earth by the quasi-static parallel electric field creating a beam-like distribution function at positive velocities.

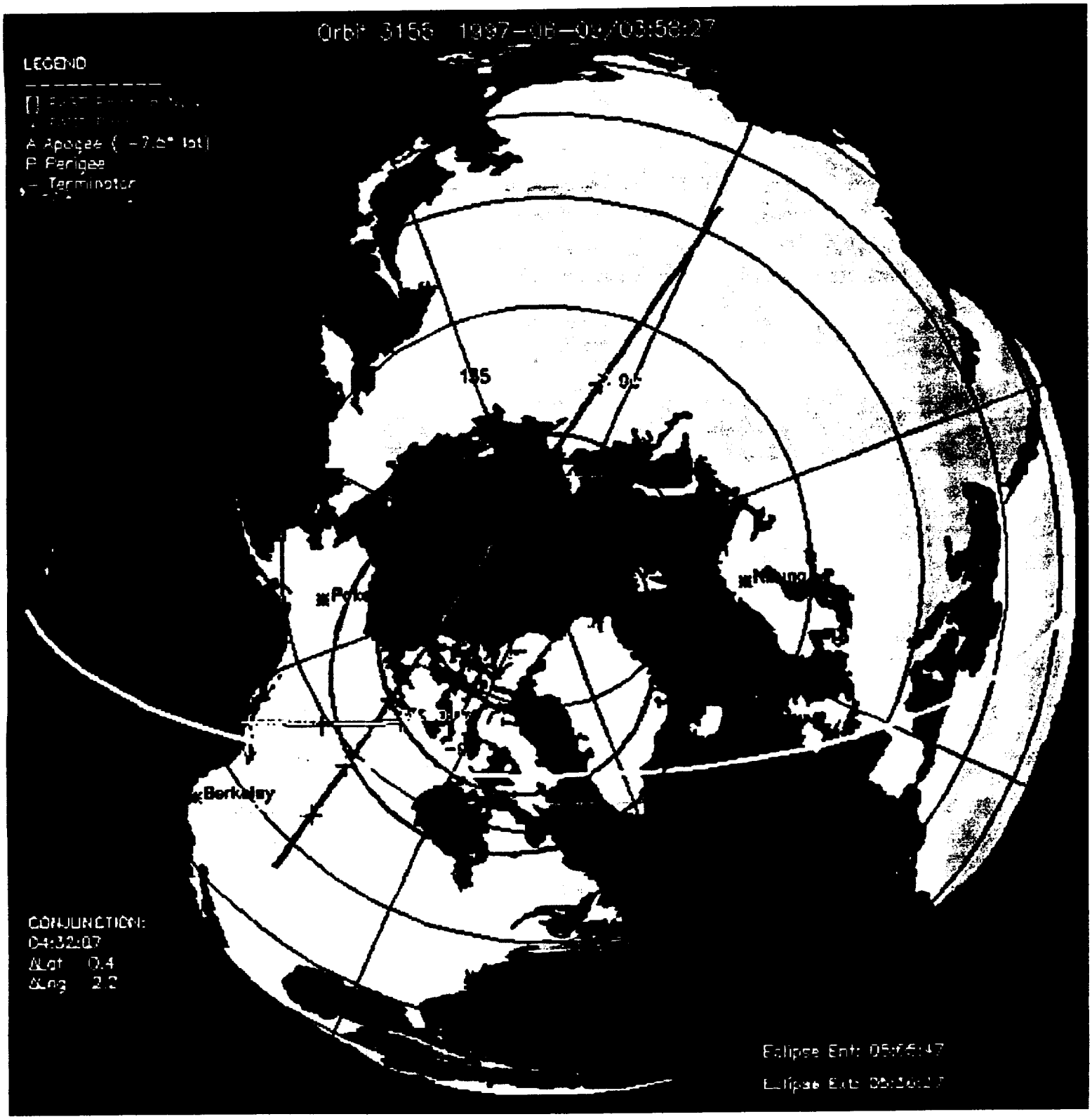
LEGEND
A Apogee (-7.6° lat)
P Perigee
Terminator
135
Berkeley
CONJUNCTION:
04:32:07
ΔLat 0.4
ΔLng 2.2

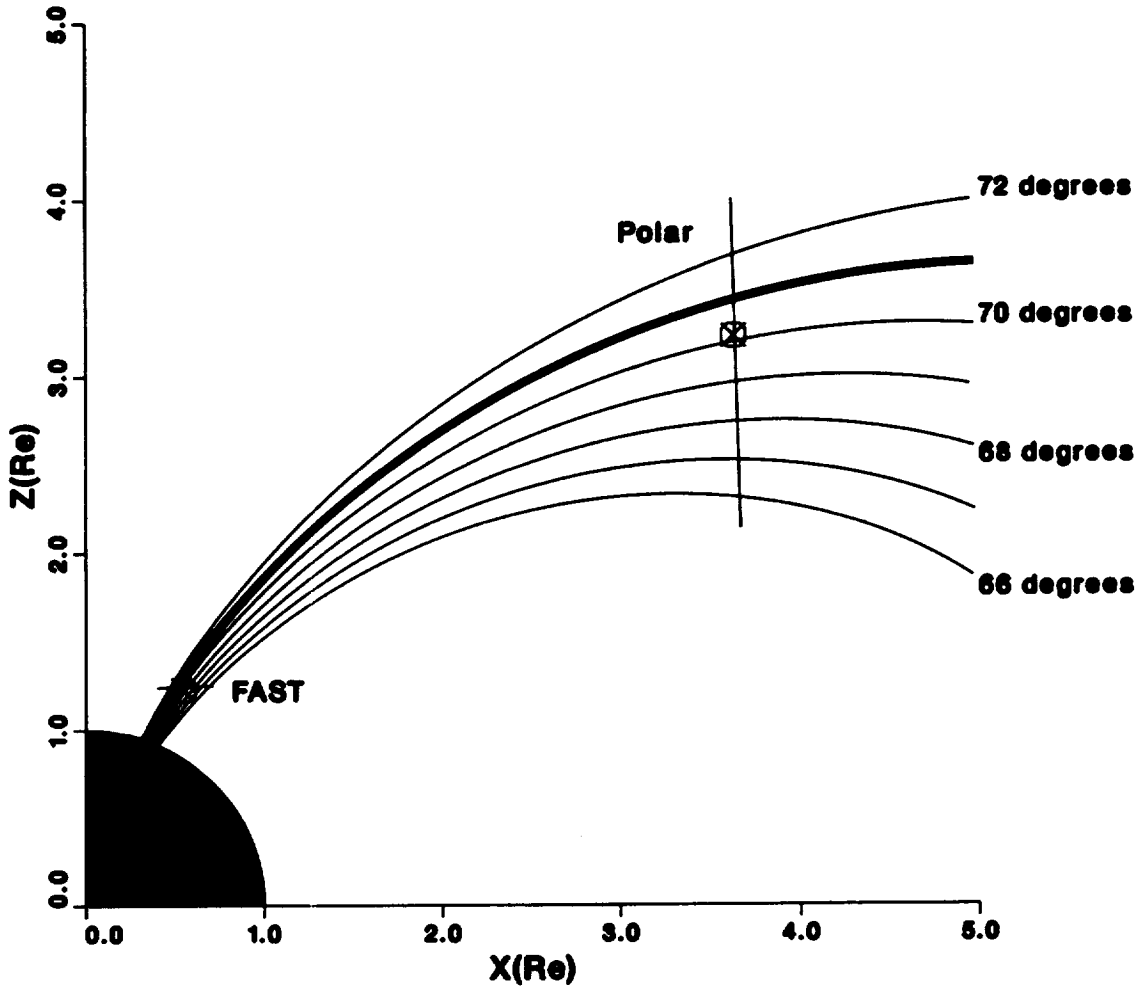
Z(Re)
X(Re)
0.0
1.0
2.0
3.0
4.0
5.0
Polar
72 degrees
70 degrees
68 degrees
66 degrees
FAST

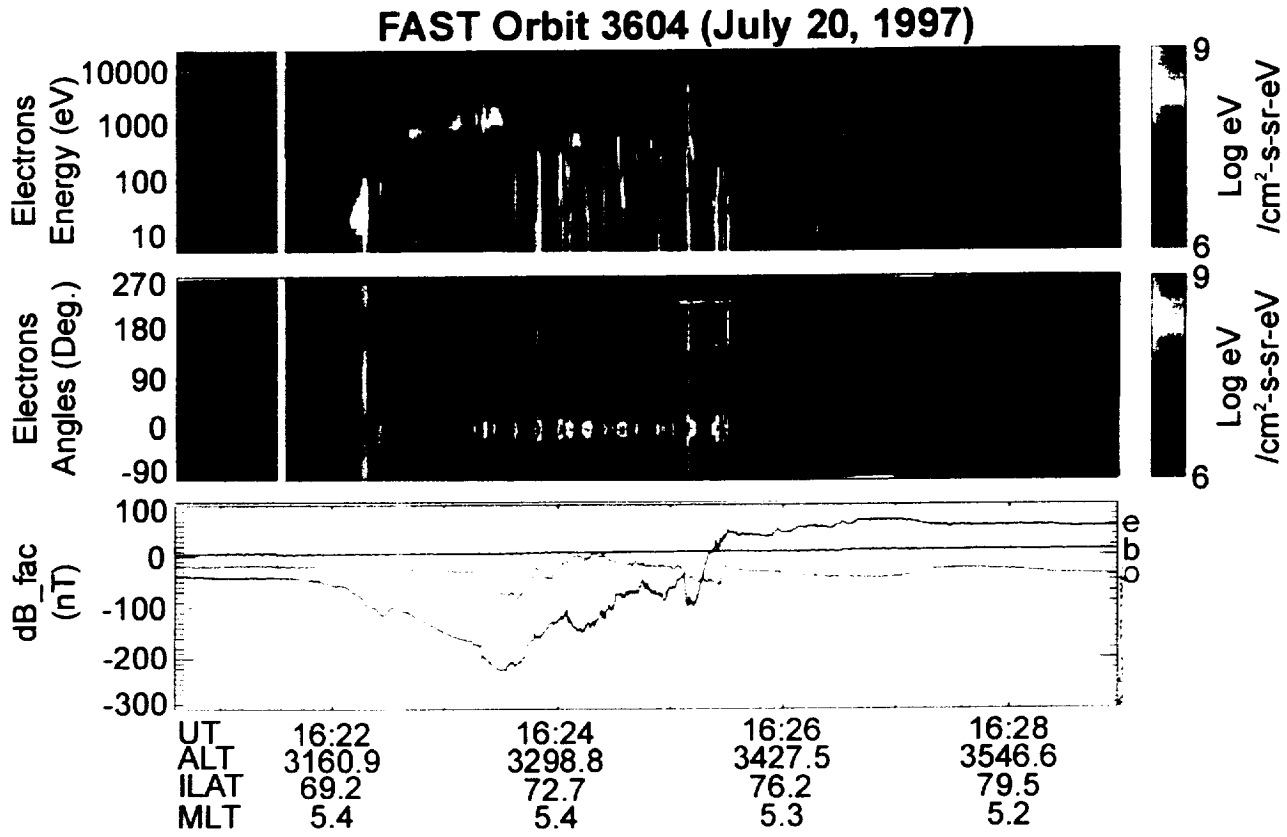
FAST Orbit 3604 (July 20, 1997)
Electrons Energy (eV)
10000
1000
100
10
9
6
Log eV /cm²-s-sr-eV
Electrons Angles (Deg.)
270
180
90
0
-90
9
6
Log eV /cm²-s-sr-eV
dB_fac (nT)
100
0
-100
-200
-300
e
b
o
UT 16:22 16:24 16:26 16:28
ALT 3160.9 3298.8 3427.5 3546.6
ILAT 69.2 72.7 76.2 79.5
MLT 5.4 5.4 5.3 5.2

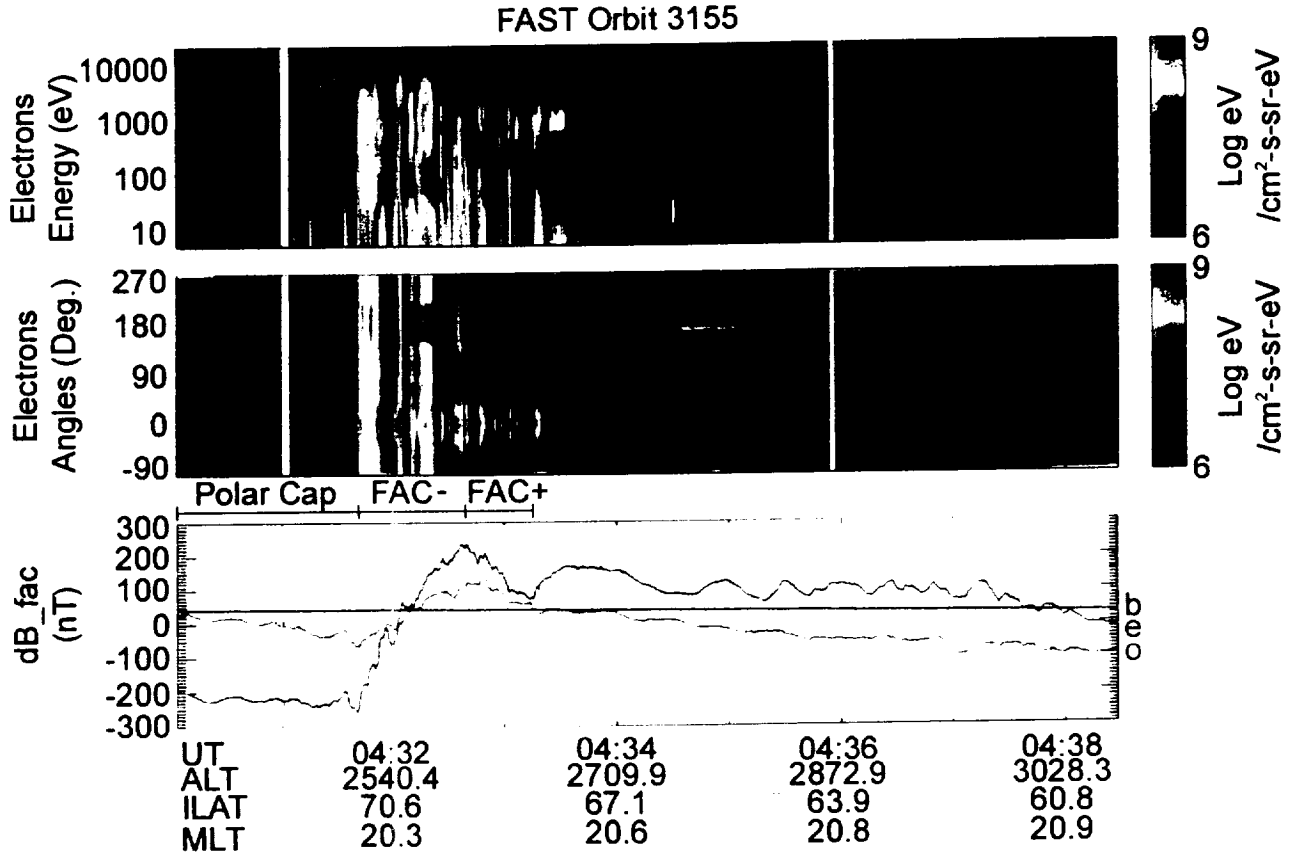
FAST Orbit 3155
Electrons Energy (eV)
10000
1000
100
10
9
6
Log eV /cm²-s-sr-eV
Electrons Angles (Deg.)
270
180
90
0
-90
9
6
Log eV /cm²-s-sr-eV
Polar Cap
FAC-
FAC+
dB_fac (nT)
300
200
100
0
-100
-200
-300
b
e
o
UT 04:32 04:34 04:36 04:38
ALT 2540.4 2709.9 2872.9 3028.3
ILAT 70.6 67.1 63.9 60.8
MLT 20.3 20.6 20.8 20.9

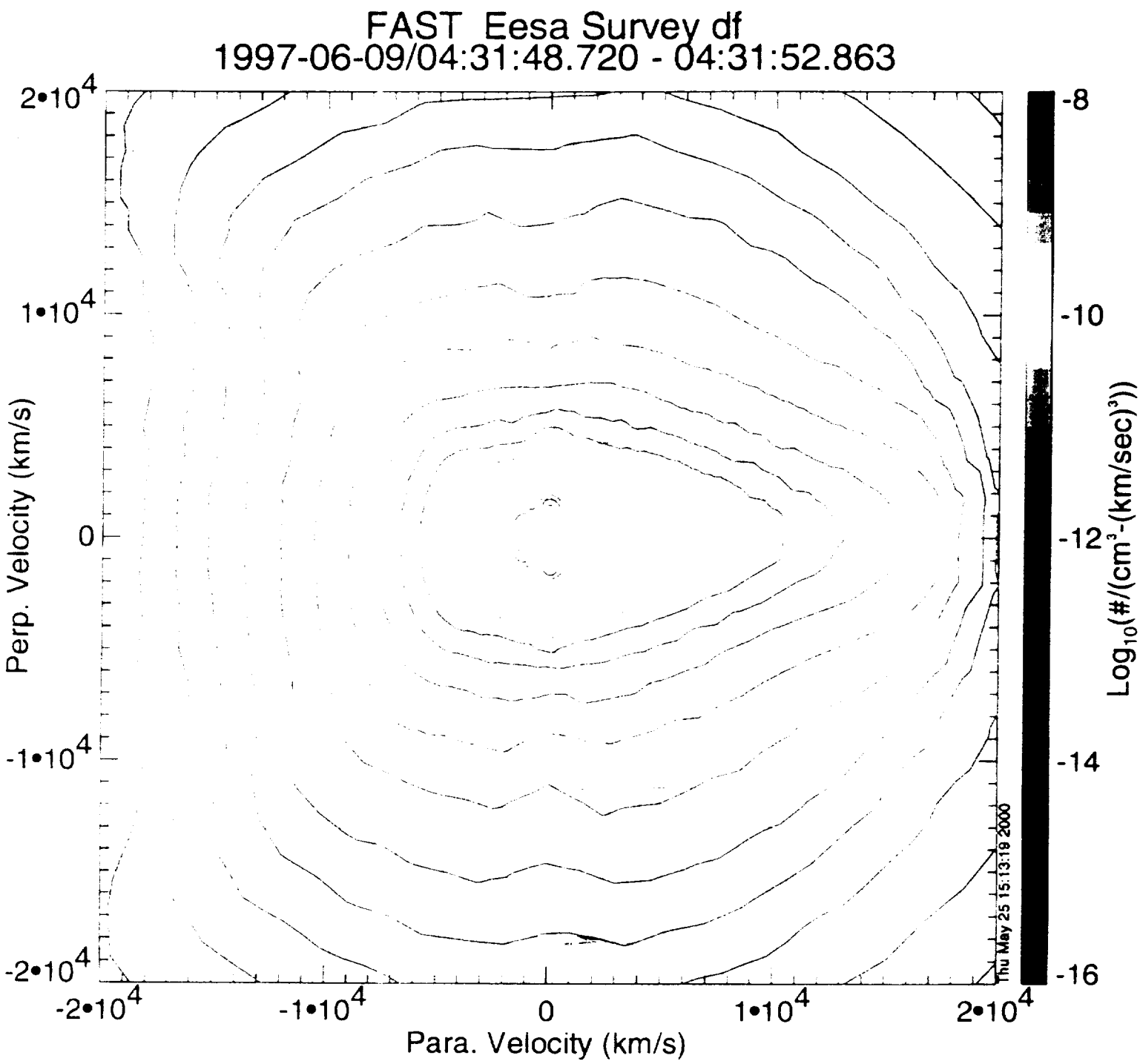
FAST Eesa Survey df
1997-06-09/04:31:48.720 - 04:31:52.863
2•10^4
1•10^4
0
-1•10^4
-2•10^4
Perp. Velocity (km/s)
-2•10^4
-1•10^4
0
1•10^4
2•10^4
Para. Velocity (km/s)
-8
-10
-12
-14
-16
Log10(#/(cm^3-(km/sec)^3))
Thu May 25 15:13:19 2000

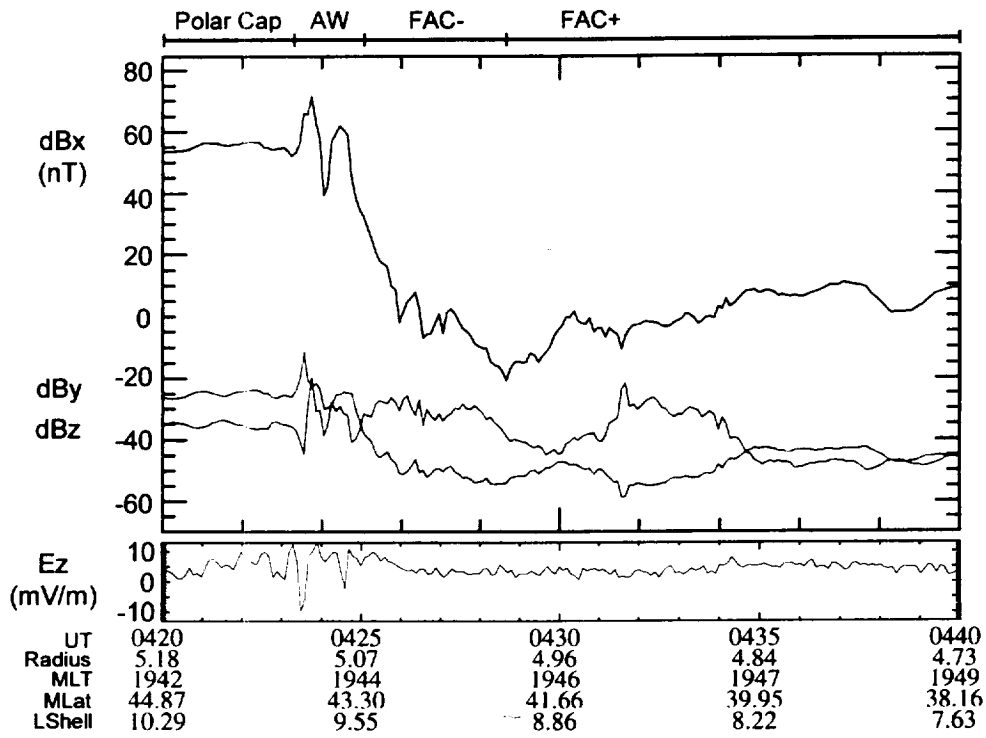
Polar Cap
AW
FAC-
FAC+
dBx
(nT)
dBy
dBz
Ez
(mV/m)
80
60
40
20
0
-20
-40
-60
10
0
-10
UT 0420 0425 0430 0435 0440
Radius 5.18 5.07 4.96 4.84 4.73
MLT 1942 1944 1946 1947 1949
MLat 44.87 43.30 41.66 39.95 38.16
LShell 10.29 9.55 8.86 8.22 7.63

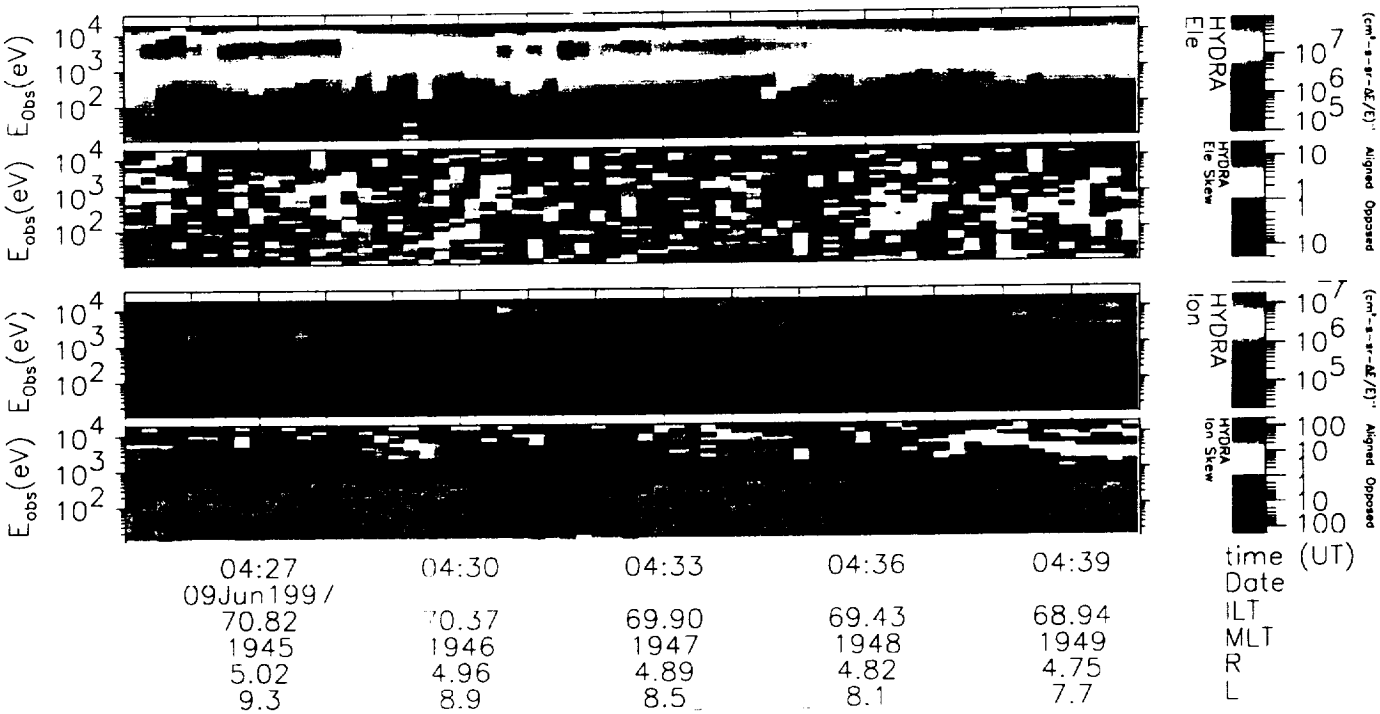
E_{obs}(eV)
10^4
10^3
10^2
HYDRA Ele
HYDRA Ele Skew
HYDRA Ion
HYDRA Ion Skew
Aligned Opposed
04:27
04:30
04:33
04:36
04:39
09Jun199 /
70.82
70.37
69.90
69.43
68.94
1945
1946
1947
1948
1949
5.02
4.96
4.89
4.82
4.75
9.3
8.9
8.5
8.1
7.7
time (UT)
Date
ILT
MLT
R
L

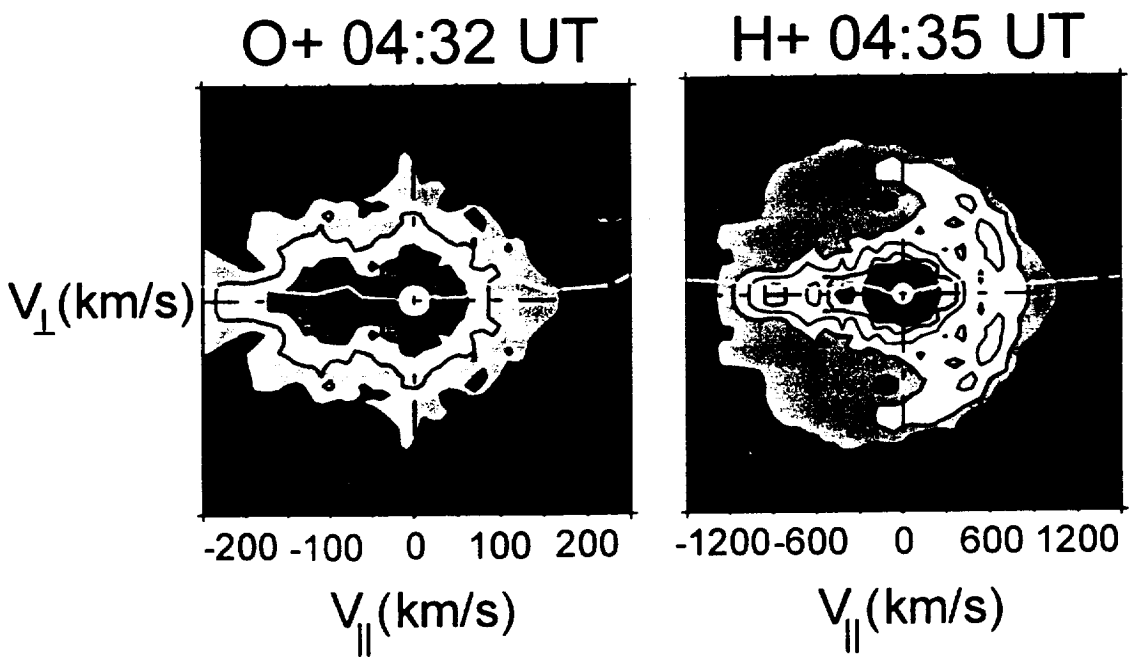
O+ 04:32 UT
H+ 04:35 UT
V⊥(km/s)
-200 -100 0 100 200
V||(km/s)
-1200-600 0 600 1200
V||(km/s)

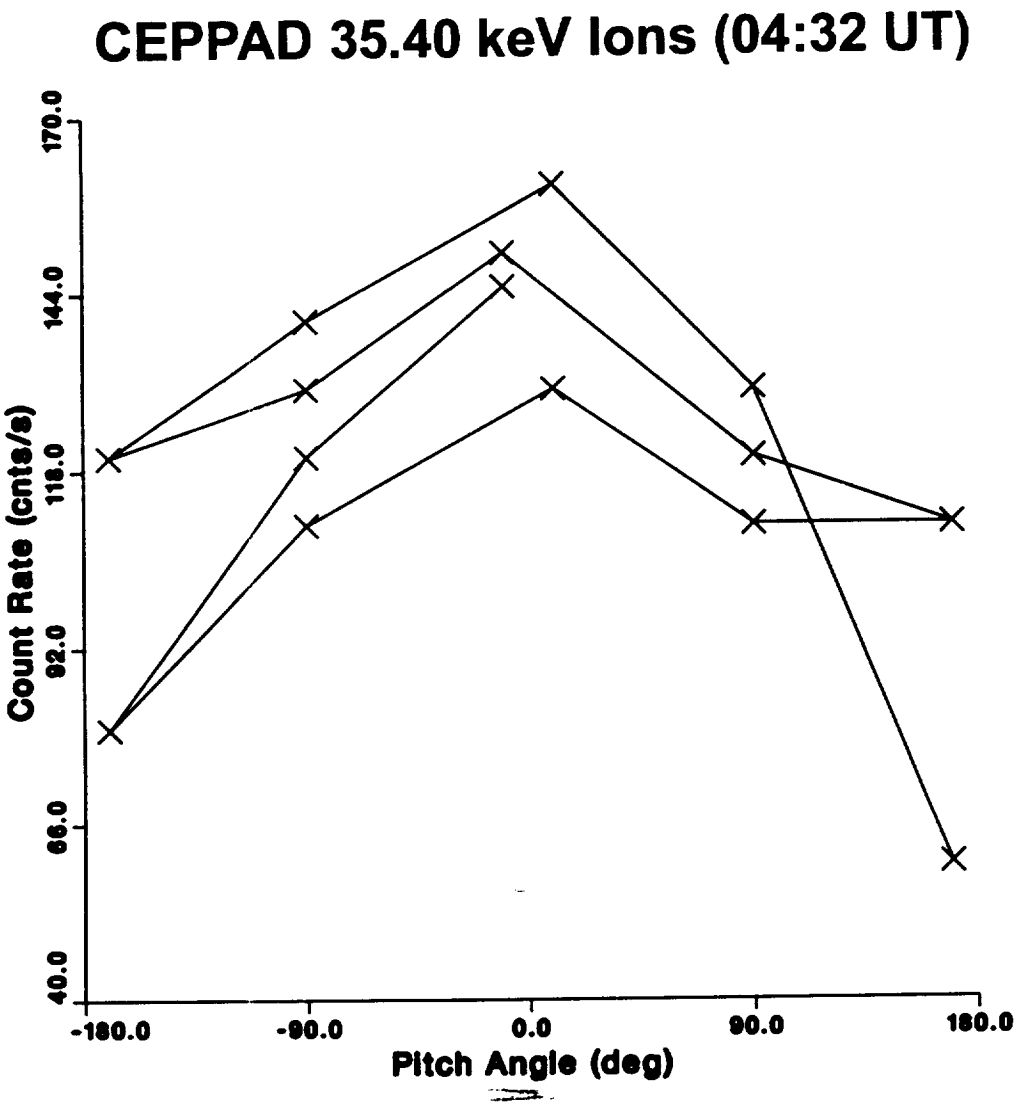
CEPPAD 35.40 keV Ions (04:32 UT)
Count Rate (cnts/s)
170.0
144.0
118.0
92.0
66.0
40.0
-180.0
-90.0
0.0
90.0
180.0
Pitch Angle (deg)

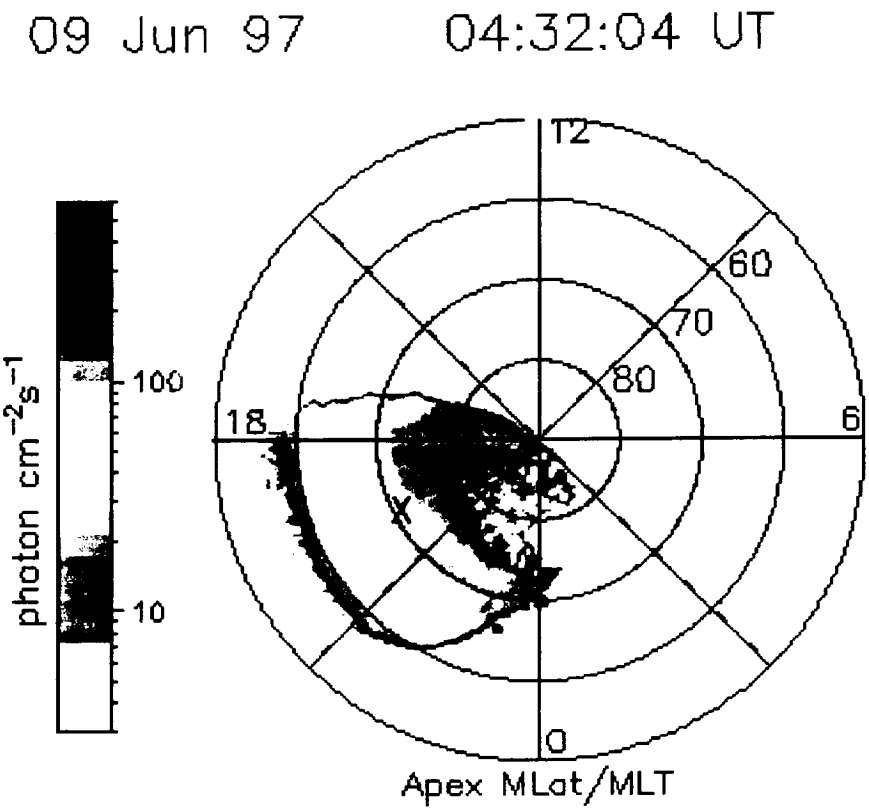
09 Jun 97
04:32:04 UT
12
60
70
80
18
6
0
100
10
photon cm^{-2}s^{-1}
Apex MLat/MLT

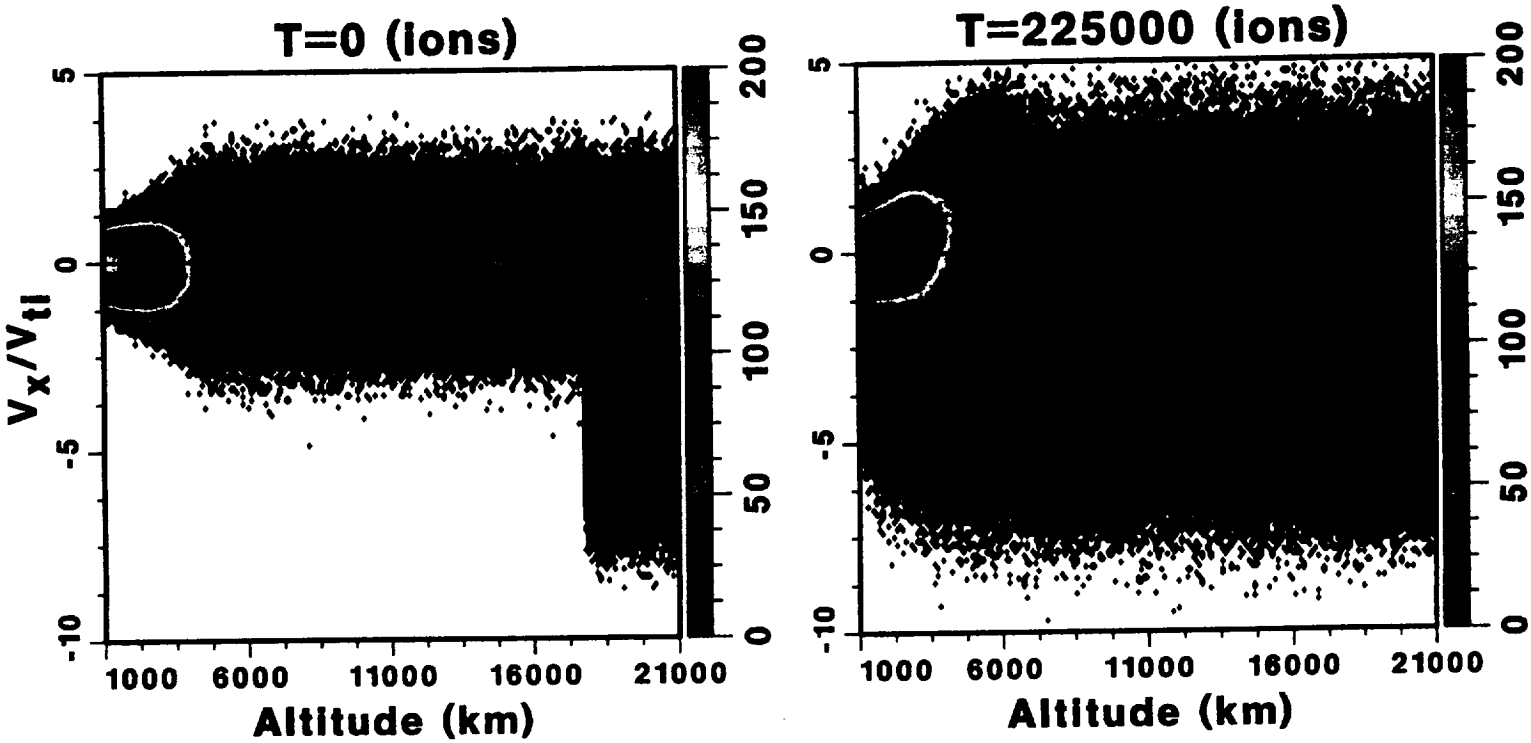
T=0 (Ions)
T=225000 (Ions)
V_x/V_{tl}
5
0
-5
-10
1000
6000
11000
16000
21000
Altitude (km)
200
150
100
50
0

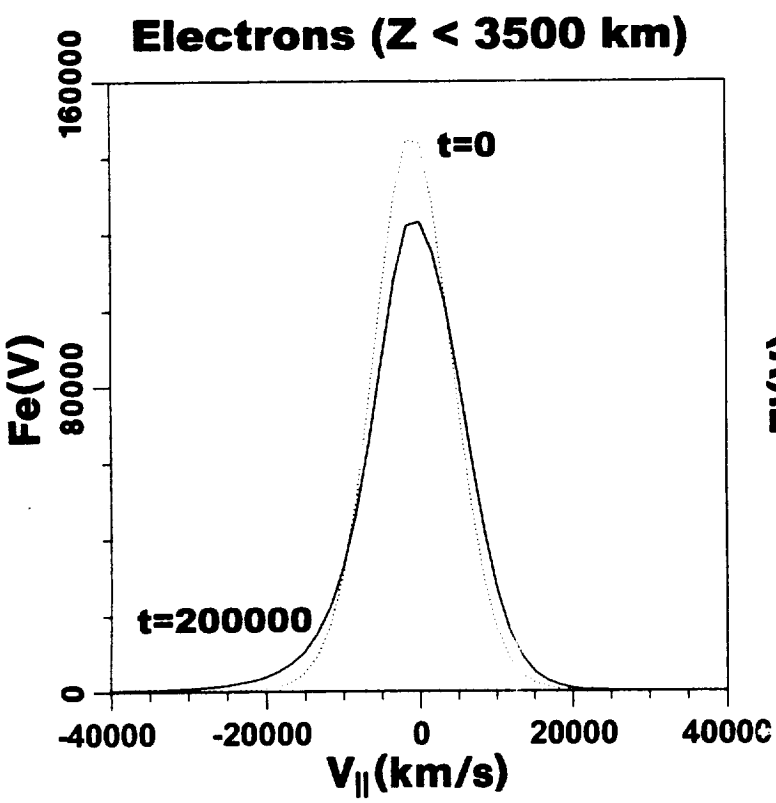
Electrons (Z < 3500 km)
160000
80000
0
Fe(V)
t=0
t=200000
-40000
-20000
0
20000
40000
V|| (km/s)

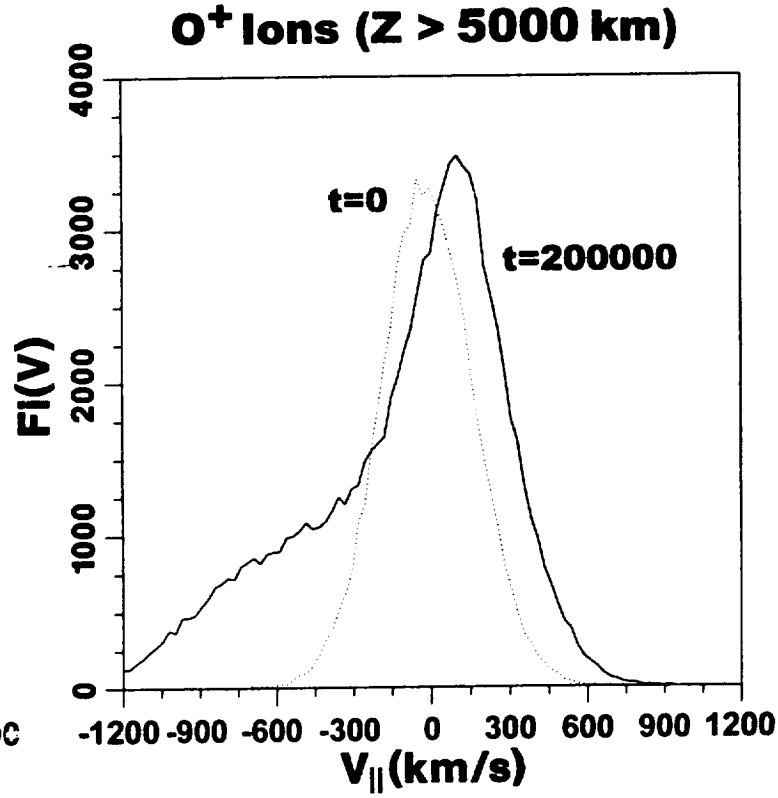
O+ Ions (Z > 5000 km)
4000
3000
2000
1000
0
FI(V)
t=0
t=200000
-1200
-900
-600
-300
0
300
600
900
1200
V|| (km/s)